The Plant Cell, Vol. 25: 944–959, March 2013, www.plantcell.org

FLYING SAUCER1 Is a Transmembrane RING E3 Ubiquitin Ligase That Regulates the Degree of Pectin Methylesterification in *Arabidopsis* Seed Mucilage[W]

Cătălin Voiniciuc,[a] Gillian H. Dean,[a] Jonathan S. Griffiths,[a] Kerstin Kirchsteiger,[b] Yeen Ting Hwang,[a,1] Alan Gillett,[a,2] Graham Dow,[a,3] Tamara L. Western,[a,4] Mark Estelle,[b] and George W. Haughn[a,5]

[a] Department of Botany, University of British Columbia, Vancouver, British Columbia V6T 1Z4, Canada
[b] Section of Cell and Developmental Biology, University of California, La Jolla, California 92093

Pectins are complex polysaccharides that form the gel matrix of the primary cell wall and are abundant in the middle lamella that holds plant cells together. Their degree of methylesterification (DM) impacts wall strength and cell adhesion since unesterified pectin regions can cross-link via Ca^{2+} ions to form stronger gels. Here, we characterize *flying saucer1* (*fly1*), a novel *Arabidopsis thaliana* seed coat mutant, which displays primary wall detachment, reduced mucilage extrusion, and increased mucilage adherence. These defects appear to result from a lower DM in mucilage and are enhanced by the addition of Ca^{2+} or completely rescued using alkaline Ca^{2+} chelators. *FLY1* encodes a transmembrane protein with a RING-H2 domain that has in vitro E3 ubiquitin ligase activity. FLY1 is orthologous to TRANSMEMBRANE UBIQUITIN LIGASE1, a Golgi-localized E3 ligase involved in the quality control of membrane proteins in yeast. However, FLY1–yellow fluorescent protein (YFP) fusions are localized in punctae that are predominantly distinct from the Golgi and the *trans*-Golgi network/early endosome in the seed coat epidermis. Wortmannin treatment, which induces the fusion of late endosomes in plants, resulted in enlarged FLY1-YFP bodies. We propose that FLY1 regulates the DM of pectin in mucilage, potentially by recycling pectin methylesterase enzymes in the endomembrane system of seed coat epidermal cells.

INTRODUCTION

Pectin is one of the most complex natural polymers and forms the dynamic gel matrix of primary cell walls in plants (Mohnen, 2008). Pectins, particularly homogalacturonan (HG) with a low degree of methylesterification (DM), are also abundant in the middle lamella, where they mediate cell–cell adhesion (Lord and Mollet, 2002; Wolf et al., 2009a). HG consists of unbranched chains of (1→4)-α-D-galacturonic acid (GalA), and rhamnogalacturonan-II has the same backbone but is a highly substituted polymer. By contrast, the rhamnogalacturonan-I (RG-I) backbone is made of alternating GalA and (1→2)-α-L-rhamnose (Rha) units that have a variable number of branches containing mainly Ara and Gal. These GalA-rich polysaccharides are proposed to form a high molecular weight complex via multiple covalent bonds (Harholt et al., 2010).

Pectin biosynthesis occurs in the Golgi and is predicted to require at least 67 different glycosyltransferases, methyltransferases, and acetyltransferases, although only a small number of enzymes are currently known and well characterized (Mohnen, 2008; Harholt et al., 2010). Analysis of GAUT1, an HG (1→4)-α-galacturonosyltransferase (Sterling et al., 2006), has recently led to the identification of a complex for HG biosynthesis with GAUT1 and GAUT7 at its core, and 12 associated proteins, including two putative pectin methyltransferases (PMTs; Atmodjo et al., 2011). Newly synthesized HG is thought to be highly methylesterified by PMTs in the Golgi, prior to being secreted to the cell wall (Zhang and Staehelin, 1992; Willats et al., 2001c; Pelloux et al., 2007). Pectin methylesterases (PMEs) in the apoplast can demethylesterify HG in a linear (blockwise) fashion, resulting in more carboxyl groups that can form bonds with Ca^{2+} ions (Moustacas et al., 1991; Goldberg et al., 1996; Wolf et al., 2009a). Linear demethylesterification is known to strengthen pectin gels, to maintain cell–cell adhesion, and to limit cell elongation (Derbyshire et al., 2007). By contrast, certain PMEs can remove methylester groups in a nonlinear manner to render HG more susceptible for degradation by polygalacturonases that facilitate cell separation (Micheli, 2001; Pelloux et al., 2007). Plant cells can also control the pectin DM by secreting PME inhibitor proteins to block the active sites of PMEs in the cell wall (Jolie et al., 2010). The analysis of novel mutants that specifically affect pectin biosynthesis or modification is necessary to increase our understanding of this complex polysaccharide (Wolf et al., 2009a).

In recent years, the *Arabidopsis thaliana* seed coat epidermis has been successfully employed as a model system for the synthesis, secretion, and modification of cell wall components,

[1] Current address: Agriculture and Agri-Food Canada, Lethbridge Research Centre, 5403 1st Ave. South, Lethbridge, Alberta T1J 4B1, Canada.
[2] Current address: EMD Inc., Suite 200, 2695 North Sheridan Way, Mississauga, Ontario L5K 2N6, Canada.
[3] Current address: Department of Biology, Stanford University, 371 Serra Mall, Stanford, CA, 94305.
[4] Current address: Department of Biology, McGill University, 1205 Dr. Penfield Ave., Montreal, Quebec H3A 1B1, Canada.
[5] Address correspondence to george.haughn@ubc.ca.
The author responsible for distribution of materials integral to the findings presented in this article in accordance with the policy described in the Instructions for Authors (www.plantcell.org) is: George W. Haughn (george.haughn@ubc.ca).
[W] Online version contains Web-only data.
www.plantcell.org/cgi/doi/10.1105/tpc.112.107888

particularly pectin (Haughn and Western, 2012). The hallmark of this cell layer is the production of three distinct cell wall structures: an outer primary wall, a pectinaceous mucilage pocket, and a cellulose-rich columella (Beeckman et al., 2000; Western et al., 2000; Windsor et al., 2000, Mendu et al., 2011). Between 5 and 8 days post anthesis (DPA), large amounts of pectin are secreted to the apoplastic space at the junction of the outer tangential and radial primary walls, forming a donut-shaped pocket of mucilage around a cytoplasmic column (Western et al., 2000; Young et al., 2008). The epidermal cells then synthesize a volcano-shaped secondary wall (9 to 11 DPA), which protrudes through the center of the mucilage pocket and connects to the primary wall. Hydration of mature seeds triggers the rapid expansion of mucilage, releasing a nonadherent layer that easily detaches from the seed and an adherent layer that can only be removed with strong acid or base treatment (Western et al., 2000; Macquet et al., 2007a). During mucilage extrusion from wild-type seeds, the outer tangential primary wall detaches from the radial wall but remains attached to the columella (Western et al., 2000, 2001; Dean et al., 2007; Macquet et al., 2007b).

Analysis of mucilage mutants has led to the identification of several genes that are involved in the biosynthesis of cell wall components. Mucilage is composed primarily of unbranched RG-I, with small quantities of HG, cellulose, and xyloglucan found in the inner adherent layer (Western et al., 2000; Macquet et al., 2007a; Young et al., 2008). Mutants that lack enzymes required for pectin biosynthesis (*mum4*, Usadel et al., 2004; Western et al., 2004; *gaut11*, Caffall et al., 2009) or for pectin modification (*mum2*, Dean et al., 2007; Macquet et al., 2007b; *sbt1.7*, Rautengarten et al., 2008; *bxl1*, Arsovski et al., 2009; *pmei6*, Saez-Aguayo et al., 2013) display reduced mucilage production and/or release. MUCILAGE-MODIFIED4 (MUM4/RHM2) is a UDP-L-rhamnose synthase required for an early step in RG-I biosynthesis (Usadel et al., 2004; Western et al., 2004; Oka et al., 2007). *BXL1* encodes an α-L-arabinofuranosidase that removes arabinan residues located on the side chains of RG-I (Arsovski et al., 2009), and *MUM2* encodes a β-D-galactosidase (BGAL6) that removes RG-I galactose side chain residues (Dean et al., 2007; Macquet et al., 2007b). Very little is known about HG synthesis in the *Arabidopsis* seed coat aside from the role of GAUT11, an α-1,4-D-galacturonosyltransferase (Caffall et al., 2009), but there is increasing evidence that establishing the correct DM of HG is essential for mucilage extrusion. Although their PME targets are currently unknown, SBT1.7, an extracellular subtilisin-like protease (Hamilton et al., 2003; Rautengarten et al., 2008), and PMEI6 (Saez-Aguayo et al., 2013) were shown to promote mucilage release by inhibiting PME activity in seed coat epidermal cells.

In addition, analysis of *cesa5*/*mum3* and *sos5* mutants revealed that cellulose and arabinogalactan proteins are involved in mucilage adherence to the seed (Harpaz-Saad et al., 2011; Mendu et al., 2011; Sullivan et al., 2011). Despite these discoveries, large gaps remain in the current knowledge of cell wall biogenesis in the seed coat.

Here, we characterize a seed coat mutant, *flying saucer1* (*fly1*), which has more compact mucilage capsules and detached outer tangential primary walls when hydrated in water. The *fly1* defects apparently result from a lower pectin DM in mucilage and can be intensified by adding Ca^{2+} ions or completely rescued by alkaline cation chelators. We show that FLY1 is a transmembrane RING E3 ubiquitin ligase, which controls the DM of pectin in seed mucilage.

RESULTS

fly1-1 Seeds Release Discs Upon Hydration in Water

The *fly1-1* mutant line was isolated by screening for seed mucilage defects in a Columbia-2 (Col-2) population mutagenized with ethyl methanesulfonate (EMS). Wild-type extruded mucilage is not homogeneous but consists of an outer, nonadherent layer that is easily removed by shaking in water and an inner, adherent layer, which remains attached to the seed even after prolonged shaking (see Supplemental Figure 1 online; Western et al., 2000; Macquet et al., 2007a). Mature wild-type seeds, shaken in water and stained with Ruthenium Red (RR), a pectin dye (Sterling, 1970), are surrounded by a pink gel-like capsule (Figure 1A). In contrast with the wild type, hydrated *fly1-1* seeds appear to release smaller mucilage halos, surrounded by a large number of darkly stained small discs (Figure 1B). The difference between wild-type and *fly1-1* mucilage halos is enhanced when dry seeds are hydrated directly in RR (see Supplemental Figures 1C and 1D online). The *fly1-1* discs appear at the periphery of the adherent mucilage layer and are not detached from the seed after 24 h of shaking with an orbital rotator (see Supplemental Figures 1E and 1F online). This suggests that the discs are strongly bound to the adherent mucilage and may result from reduced mucilage extrusion in *fly1-1* compared with the wild type. Although mucilage must be stained to be clearly observed (Figure 1C), the *fly1-1* discs are also visible without staining, suggesting that they cannot be composed solely of mucilage (Figure 1D).

Primary Cell Walls Detach From *fly1-1* Seed Coat Epidermal Cells

Mature seed coat epidermal cells contain three morphologically and chemically distinct cell walls (Western et al., 2000; Macquet et al., 2007a; Young et al., 2008). The *fly1-1* discs resemble the polygonal shape of the outer tangential primary walls, which are normally attached to the columellae of hydrated seeds (Western et al., 2004; Dean et al., 2007; Stork et al., 2010). We therefore examined the position of the outer primary walls in wild-type and *fly1-1* seeds shaken in water. All wild-type seed epidermal cells have primary walls attached to their columellae, but many *fly1-1* cells display columellae with no attached walls (see Supplemental Figures 1G and 1H online). We further investigated the composition of the *fly1-1* discs using Pontamine Fast Scarlet 4B (S4B), which preferentially stains cellulose microfibrils (Anderson et al., 2010). All wild-type seed coat epidermal cells have S4B-stained primary wall fragments attached to their columellae (Figures 1E and 1G), consistent with the observations made using unstained seeds in water. Although wild type and *fly1-1* have similar levels of diffuse S4B labeling in the inner mucilage layers, *fly1-1* seeds display many S4B-stained discs, which are at the outer edge of the mucilage halo and are positioned above columellae that lack S4B-labeled primary wall attachment (Figures 1F and 1H).

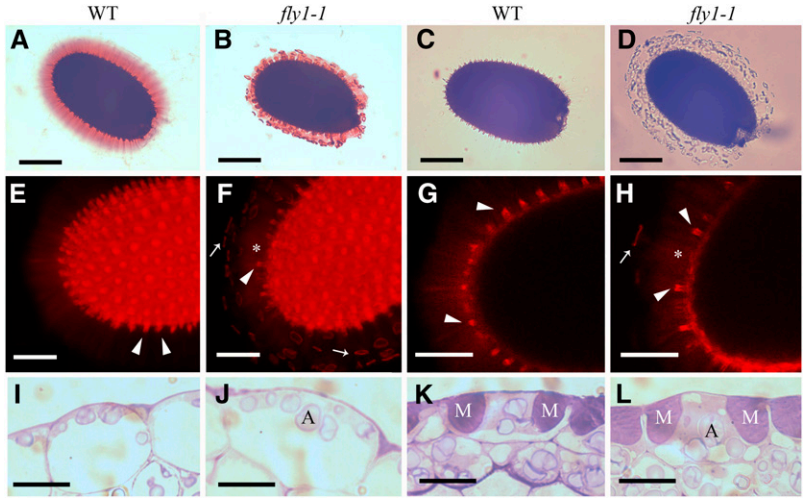

Figure 1. *fly1-1* Seeds Display Primary Wall Detachment and Reduced Mucilage Extrusion.

(A) and **(B)** Mature seeds shaken in water for 2 h and stained with RR. The mucilage capsule of *fly1-1* is smaller than the wild type (WT) and is surrounded by disc-like structures.
(C) and **(D)** Mature seeds shaken in water for 2 h. The *fly1-1* discs, unlike mucilage, can be clearly seen without staining.
(E) to **(H)** Mature seeds shaken in water for 2 h and stained with S4B.
(E) and **(F)** S4B signal from multiple optical slices.
(G) and **(H)** Optical slices through the middle of seeds. Arrowheads indicate S4B-labeled primary cell walls attached to columellae. The loss of primary wall attachment (asterisk) correlates with the position of *fly1-1* discs (arrow).
(I) to **(L)** The development of *fly1-1* seed coat epidermal cells is indistinguishable from the wild type at 4 DPA (**[I]** and **[J]**) and 7 DPA (**[K]** and **[L]**). M, mucilage pockets. A, amyloplasts.
Bars = 200 μm in **(A)** to **(D)**, 100 μm in **(E)** to **(H)**, and 15 μm in **(I)** to **(L)**.

The surface morphology of wild-type and *fly1-1* dry seeds was examined by scanning electron microscopy (SEM). Wild-type and *fly1-1* seed epidermal cells displayed outer tangential cell walls and columellae with similar shapes and sizes (Figures 2A and 2B). To investigate the structure of extruded mucilage, seeds hydrated in water were immediately frozen in liquid nitrogen and examined with cryo-scanning electron microscopy (cryoSEM). Both wild-type and *fly1-1* hydrated seeds display intricate mesh-like networks of mucilage (Figures 2C to 2F). However, only the mutant seeds show electron-dense discs on top of the extruded mucilage matrix (Figures 2D and 2F), consistent with position of RR-stained discs at the edge of the *fly1-1* mucilage halo (Figure 1B). Since the outer primary cell walls viewed with SEM (Figure 2B) and the *fly1-1* discs observed with cryoSEM (Figures 2D and 2F) or RR staining (Figure 1B) resemble polygons, we measured their diameters (>30 samples per technique) and compared them using Student's *t* tests. The diameter of *fly1-1* outer tangential primary walls observed with SEM (32.95 ± 0.69 μm; mean ± SE) is similar to that of RR-stained discs (32.98 ± 0.88 μm; $P = 0.98$). The cryoSEM discs (30.88 ± 0.70 μm) are similar to RR-stained discs ($P = 0.066$, >0.05) but significantly smaller than walls in SEM micrographs ($P = 0.038$, <0.05).

Analysis of hydrated seeds prior to and after S4B staining revealed that *fly1-1* discs contain cellulose and are positioned above columellae lacking attached primary walls. The *fly1-1* discs in light and cryoSEM micrographs were similar in size to the primary walls of the seed coat epidermis visualized with SEM. Overall, the results in this section strongly support the hypothesis that the outer tangential primary cell walls of many *fly1-1* seed coat epidermal cells detach from columellae upon mucilage extrusion in water.

fly1 Seeds Have Normal Development and Monosaccharide Composition

To determine if the *fly1-1* mucilage extrusion defects result from abnormal seed coat differentiation, fixed sections of developing seeds were analyzed using light microscopy. The development of *fly1-1* seed epidermal cells is indistinguishable from the wild type and mucilage biosynthesis appears unaffected (Figures 1I to 1L), unlike mutants that synthesize less pectin, such as *mum4* (Western et al., 2004). Primary wall attachment to the columella appears identical to the wild type in live *fly1-1* seed coat epidermal cells at 12 DPA (see Supplemental Figures 1I and 1J online). The unaltered development of *fly1-1* seed coat cells is consistent with the normal surface morphology of dry mature seeds (Figures 2A and 2B).

The monosaccharide composition of wild-type and *fly1-1* whole seeds was determined using high-performance anion-exchange chromatography (HPAEC). The alcohol-insoluble residues (AIRs) prepared from *fly1-1* and wild-type seeds contained similar monosaccharide levels (Table 1), consistent with seed coat mutants that primarily affect pectin modification rather than pectin biosynthesis (Dean et al., 2007; Arsovski et al., 2009). Overall, the *fly1-1* seed development and the whole seed HPAEC results

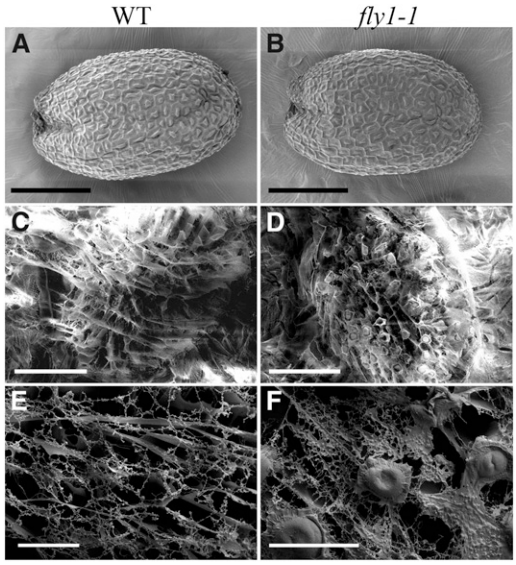

Figure 2. Analysis of Dry and Hydrated Seeds by Scanning Electron Microscopy and Cryo-Scanning Electron Microscopy.

(A) and **(B)** The surface morphology of dry mature *fly1-1* seeds viewed with scanning electron microscopy is indistinguishable from the wild type (WT).

(C) to **(F)** Cryo-scanning electron microscopy of mucilage extruded from mature seeds hydrated in water. Wild-type seeds showed an irregular mucilage matrix before **(C)** and after sputter coating **(E)**. *fly1-1* seeds have discs on top of the mucilage matrix before **(D)** and after sputter coating **(F)**.

Bars = 200 μm in **(A)** to **(D)** and 50 μm in **(E)** and **(F)**.

suggest that *FLY1* is not required for the biosynthesis of a major cell wall polysaccharide.

fly1 Mucilage Is More Adherent Than Wild-Type Mucilage

We investigated if *FLY1* affects mucilage extrusion and adhesion by analyzing the monosaccharide compositions of sequential mucilage extractions from wild-type and *fly1-1* seeds. Although *fly1-1* discs are not detached from the seed by gentle shaking, vigorous agitation using a vortex mixer can remove the majority of polygonal discs and the adherent mucilage (see Supplemental Figure 2 online). Therefore, we extracted mucilage without discs by gently shaking seeds in water for 1 h, followed by mucilage including discs by vigorously shaking in water for an additional 2 h.

HPAEC monosaccharide analysis of the first mucilage extraction showed a strong reduction of Rha and GalA in *fly1-1* mucilage relative to the wild type, but the subsequent *fly1-1* mucilage extraction contained almost twice as much Rha and GalA compared with the wild type (Table 1). All other monosaccharides detected are minor mucilage components, but showed similar trends to Rha and GalA.

In addition to the sequential extractions, total mucilage amounts were extracted from water-hydrated seeds by adding NaOH to a final concentration 0.2 M and vortex mixing for 1 h. No RR-stained mucilage remained around wild-type and *fly1-1* seeds (see Supplemental Figures 2K and 2L online). Wild-type and *fly1-1* mucilage extracted by NaOH have similar monosaccharide compositions (see Supplemental Figure 2M online).

Despite having whole seed and total mucilage monosaccharide compositions similar to the wild type, *fly1-1* seeds display a reduced mucilage extractability in water. The *fly1-1* mucilage capsule is more adherent than the wild type since vigorous shaking in water partially compensates for the reduced monosaccharide levels in the first *fly1-1* water extraction.

The *fly1* Mucilage Defects Are Calcium and pH Dependent

Similar to the wild type, *fly1-1* seeds release a mucilage halo within 10 s of hydration in water (see Supplemental Figure 3 online). However, *fly1-1* discs continue to be released after more than 60 s (see Supplemental Figure 3D online), suggesting that some *fly1-1* cells have delayed mucilage release. Compared with the wild type, *fly1-1* seeds have a more compact and adherent mucilage halo (Figures 3A and 3B, Table 1). To identify the cause of reduced mucilage expansion in the *fly1-1* mutant, we examined the effects of hydrating seeds in a $CaCl_2$ solution. Ca^{2+} ions are required for the formation of cross-links between unesterified HG blocks and can therefore strengthen the pectin gel matrix (Jarvis, 1984). Interestingly, hydration of seeds directly in 50 mM $CaCl_2$ almost completely impairs mucilage extrusion from the *fly1-1* mutant but not from wild-type seeds, which show only a small reduction in mucilage halo size (Figures 3C and 3D). This suggests that pectins in *fly1-1* mucilage can form more calcium cross-links than in the wild type. Although only a few $CaCl_2$-treated *fly1-1* seed epidermal cells release mucilage, all of these appear to have discs atop their compact mucilage columns (Figure 3D, inset).

In stark contrast with the addition of Ca^{2+} ions, cation chelators such as EDTA can disrupt cross-links between unesterified HG chains and facilitate seed mucilage extrusion (Rautengarten et al., 2008; Arsovski et al., 2009). Hydration of mature seeds in 50 mM EDTA pH 8.0 completely rescued the *fly1-1* mucilage extrusion defect, resulting in equally large wild-type and *fly1-1* mucilage capsules without any visible discs (Figures 3E and 3F). RR-stained discs were not observed in EDTA-hydrated *fly1-1* seeds (Figure 3F), indicating that EDTA may also rescue the primary wall detachment phenotype of this mutant. Surprisingly, unstained *fly1-1* seeds hydrated directly in EDTA look identical to wild-type seeds and have primary cell wall fragments attached to all columellae (Figures 3G and 3H). S4B staining confirmed that the primary walls stay attached to columellae in *fly1-1* seeds hydrated with EDTA (Figures 3I and 3J).

Since pectin is stabilized at acidic pH and can be degraded at alkaline pH (Sriamornsak, 2003), we investigated if the suppression of the *fly1-1* mucilage defects is also pH dependent. The EDTA pH 6.0 treatment largely rescued the *fly1-1* defects similar to EDTA pH 8.0 (see Supplemental Figures 4A to 4C online). Treatment with 50 mM HEPES buffer, which does not bind Ca^{2+}, partially rescued the *fly1-1* defects at pH 8.0 but not at pH 6.0 (see Supplemental Figures 4D to 4F online). Seeds treated with both EDTA and HEPES resembled the EDTA-treated seeds (see Supplemental Figures 4G to 4I online). Removal of Ca^{2+} by EDTA is largely sufficient to rescue the *fly1-1* mucilage defects, but an alkaline pH also contributes to rescue the mutant phenotype.

Table 1. Monosaccharide Composition of Sequentially Extracted Mucilage and Whole Seeds

	Mucilage Extraction 1		Mucilage Extraction 2		Whole Seeds	
Sugar	Wild Type	*fly1-1*	Wild Type	*fly1-1*	Wild Type	*fly1-1*
Fuc	Trace	Trace	Trace	Trace	4.03 ± 0.20	3.98 ± 0.17
Ara	1.03 ± 0.80	0.67 ± 0.12	0.35 ± 0.01	0.35 ± 0.05	182.30 ± 5.75	170.40 ± 5.40
Rha	46.92 ± 1.18	26.60 ± 2.72	12.27 ± 1.66	19.69 ± 1.83	192.38 ± 8.52	174.88 ± 5.49
Gal	2.35 ± 0.16	1.14 ± 0.15	0.64 ± 0.10	1.06 ± 0.09	110.58 ± 3.98	100.48 ± 3.19
Glc	1.20 ± 0.18	0.77 ± 0.07	0.80 ± 0.19	0.93 ± 0.11	178.62 ± 13.04	179.46 ± 6.17
Xyl	2.76 ± 0.05	1.96 ± 0.32	0.63 ± 0.12	1.50 ± 0.12	48.51 ± 1.26	48.43 ± 2.94
GalA	58.67 ± 0.60	33.70 ± 3.86	13.74 ± 2.38	26.40 ± 2.26	312.89 ± 14.34	313.02 ± 7.37

Extraction 1 (gently shaking in water for 1 h) contains mucilage without discs, while extraction 2 (an additional 2 h of vigorously shaking in water) includes both mucilage and discs (see Supplemental Figure 2 online). Values are the mean ± SE of four (mucilage) or three samples (whole seed) and represent nmol sugar per milligram seed used for mucilage extraction or milligram alcohol-insoluble residue hydrolyzed (whole seed). Results were verified using two additional biological replicates.

The *fly1* Mucilage Has More Unesterified HG Than the Wild Type

Since the *fly1-1* defects are sensitive to the presence of Ca^{2+} ions, *fly1-1* mucilage likely contains more unesterified GalA than wild-type mucilage. Immunolabeling of mature seeds with three anti-HG antibodies was conducted to determine if *fly1-1* mucilage displays an altered pattern of methylesterification. The same image acquisition settings were used within each immunolabeling experiment. 2F4, an antibody that specifically binds unesterified blocks of HG cross-linked by Ca^{2+} ions (Liners et al., 1989), only labeled primary cell wall material in wild-type seeds (Figure 4), including the outer tangential walls attached to columellae and the radial walls. Interestingly, *fly1-1* seeds displayed 2F4 signal in both the primary cell wall and in the extruded mucilage. The abundance of 2F4 signal in *fly1-1* mucilage, along its absence in wild-type mucilage, is consistent with increased amounts of unesterified HG in the mutant.

Two additional antibodies with broader specificities were also used to characterize the seed mucilage: JIM7, which binds to heavily (35 to 81%) methylesterified HG (Knox et al., 1990), and JIM5, which binds partially (up to 40%) methylesterified HG (Vandenbosch et al., 1989). JIM5 and JIM7 recognize partially overlapping domains of seed mucilage and both labeled larger regions of *fly1-1* mucilage compared with the wild type (see Supplemental Figure 5 online). The results of all three antibodies are consistent with *fly1-1* mucilage containing more unesterified HG than the wild type.

To exclude the possibility that increased immunolabeling of *fly1-1* mucilage results from higher epitope accessibility rather than larger amounts of unesterified HG, the DM of mucilage and whole seeds was determined using biochemical assays. The DM was calculated as a percentage molar ratio of methanol released after cell wall saponification (Lionetti et al., 2007) to uronic acids measured using the *m*-hydroxydiphenyl assay (van den Hoogen et al., 1998). Mucilage was extracted by vigorously shaking seeds in 50 mM EDTA for 1 h (see Supplemental Figures 2I and 2J online). Whereas wild-type and *fly1-1* whole seeds contain pectin with a similar DM (Student's *t* test, P = 0.60, >0.05), *fly1-1* mucilage has a significantly lower DM than wild-type mucilage (Student's *t* test, P = 0.02, <0.05; Figure 4F). The lower DM in *fly1-1* mucilage corroborates the increased 2F4 immunolabeling of unesterified HG (Figures 4B and 4D) and accounts for the strong effects of $CaCl_2$ and EDTA treatments on *fly1-1* mucilage defects (Figure 3). Since the altered DM appears to be the primary defect of *fly1-1* mucilage, the detached discs may result from increased binding of mucilage to the primary wall. Along with the normal DM and monosaccharide composition in *fly1-1* whole seeds (Figure 4F, Table 1), these results suggest that FLY1 is required to establish the correct DM in seed mucilage.

Cloning of the *FLY1* Gene and Expression Analysis

The *fly1-1* phenotype was shown to segregate as a single recessive nuclear mutation (3 wild type:1 *fly1*; $\chi^2 = 0.333$; $P > 0.5$; $n = 169$). The position of the *fly1-1* mutation was mapped to a 180-kb region containing 60 genes near the end of chromosome IV. We screened nearly 100 independent T-DNA insertions in 58 of the 60 candidate genes for mucilage defects. Five lines, *fly1-2* (SALK_067290), *fly1-3* (SALK_144822), *fly1-4* (SALK_139156), *fly1-5* (SALK_000015), and *fly1-6* (SALK_062423), all contained mutations in At4g28370 (Figure 5A) and produced seeds that release compact mucilage halos and discs (see Supplemental Figure 6 online). PCR-based segregation analysis using these five independent lines indicated that the T-DNA insertions were responsible for the *fly1* phenotype and were consistent with recessive loss-of-function mutations.

The At4g28370 gene encodes a previously uncharacterized protein belonging to the Really Interesting New Gene (RING) finger superfamily (TAIR 10; Lamesch et al., 2012). Sequencing of At4g28370 in the *fly1-1* background revealed a G-to-A transition, consistent with EMS mutation, at 3903 bp that changes the amino acid Trp (residue 460) to a stop codon. This early stop codon is predicted to truncate the peptide encoded by the *FLY1* gene, resulting in the loss of the conserved RING domain.

The *fly1-2* and *fly1-3* alleles were characterized in greater detail and were shown to be indistinguishable from *fly1-1* with cryoSEM, S4B staining, and anti-HG immunolabeling (data not shown). Complementation tests between *fly1-1*, *fly1-2*, and *fly1-3* failed to rescue the mucilage defects, consistent with mutations occurring in the same gene. In addition, we performed molecular complementation of *fly1-1* with a $FLY1_{pro}$:*FLY1-YFP* (Yellow

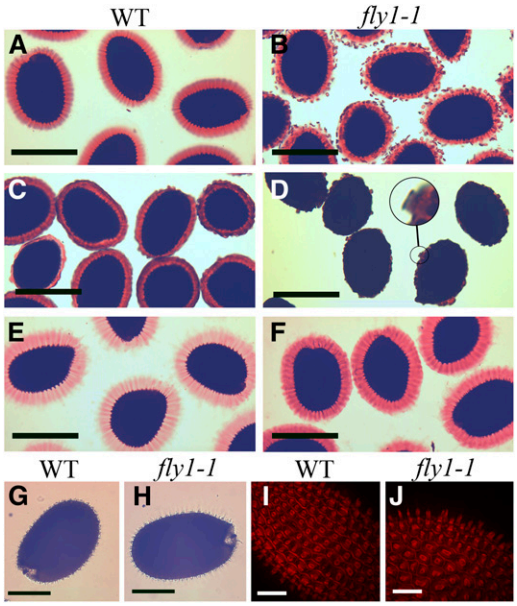

Figure 3. Effects of Ca^{2+} and EDTA on *fly1-1* Mucilage Extrusion.

(A) to **(F)** Mature seeds shaken for 45 min in water (**[A]** and **[B]**), 50 mM $CaCl_2$ (**[C]** and **[D]**), or 50 mM EDTA (**[E]** and **[F]**) and then stained with RR. Only a few $CaCl_2$-treated *fly1-1* cells release mucilage, but these appear to have discs atop compact mucilage columns (**[D]**, inset). EDTA-treated wild-type (WT) and *fly1-1* seeds have equally large mucilage capsules.

(G) and **(H)** Unstained wild-type and *fly1-1* seeds shaken in EDTA have primary walls attached to all columellae and do not display discs.

(I) and **(J)** S4B staining confirms that the columellae of EDTA-hydrated seeds have primary cell walls attached to them. Note the absence of *fly1-1* discs (**[H]** and **[J]**).

Bars = 200 μm in **(A)** to **(F)**, 150 μm in **(G)** and **(H)**, and 75 μm in **(I)** and **(J)**.

Fluorescent Protein) construct, containing wild-type At4g28370 genomic DNA (from 1 kb upstream of the ATG site to, but not including, the stop codon) fused to citrine YFP in the pAD vector (DeBono, 2012). Multiple independent *fly1-1* lines transformed with *FLY1*$_{pro}$*:FLY1-YFP* produced seeds that resemble the wild type (Figure 5B), but *fly1-1* plants transformed with empty pAD vector produced seeds that still released many discs (Figure 5C).

Consistent with the seed mucilage defects of the *fly1* mutant alleles, the Electronic Fluorescent Pictograph browser (eFP; Winter et al., 2007) revealed very high *FLY1* transcript levels in seeds relative to other *Arabidopsis* organs and preferential expression in the seed coat compared with the endosperm and embryo (Schmid et al., 2005; Le et al., 2010). Interestingly, FLY1 has one paralog in *Arabidopsis* (*FLY2*, At2g20650) and at least one ortholog in fungi, protists, green algae, mosses, and other vascular plant species with a sequenced genome (Ostlund et al., 2010; Goodstein et al., 2012; Van Bel et al., 2012). *FLY2* encodes a protein with 84.5% amino acid identity to FLY1 (Huang and Miller, 1991). Although *FLY2* transcripts are less abundant than *FLY1* in developing seeds (Zimmermann et al., 2004; Winter et al., 2007; Le et al., 2010), *FLY2* shows preferential expression in the seed coat compared with other seed tissues. To investigate if *FLY2* is also involved in mucilage biosynthesis, we isolated homozygous *fly2-1* (SALK_140887), *fly2-2* (SALK_023653), *fly2-3* (SALK_074297), *fly2-4* (SAIL_515_C07), and *fly2-5* (WiscDsLox412F02) T-DNA lines (see Supplemental Figure 7 online). Hydrated *fly2* seeds display wild-type RR staining (see Supplemental Figure 6 online), S4B staining, and 2F4, JIM5, and JIM7 immunolabeling (data not shown).

The function of *FLY1* and *FLY2* may not be limited to the seed coat since RT-PCR analysis detected the highest transcript levels in stems (Figure 5D). According to multiple microarray data sets, both genes are most strongly expressed in stem and root xylem cells (see Supplemental Figure 8A online; Brady et al., 2007; Hruz et al., 2008), suggesting that they may play a role in vasculature development. However, neither *fly1* nor *fly2* mutants show any obvious defects in leaf, stem, or root morphology. In the GeneCAT

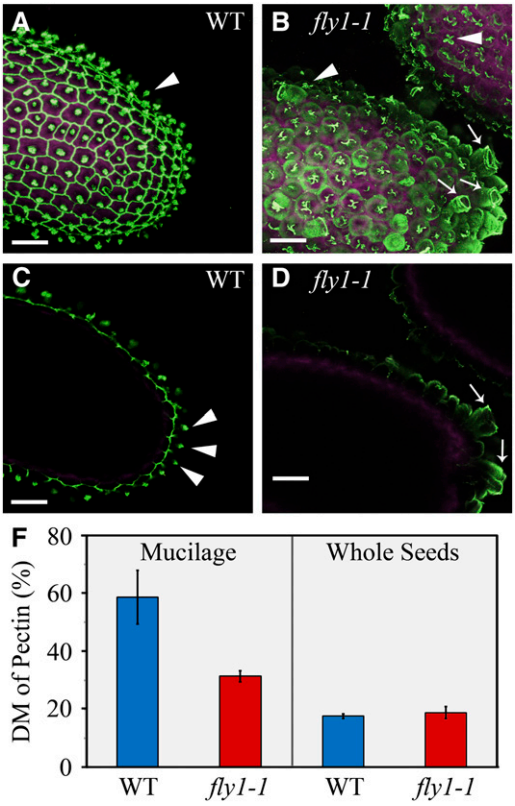

Figure 4. Immunolabeling and Biochemical Analysis of Pectin DM in Seeds and Mucilage.

(A) to **(D)** 2F4 immunolabeling (green) of unesterified HG and seed intrinsic fluorescence (magenta).

(A) and **(B)** Maximum intensity signals from multiple optical stacks.

(C) and **(D)** Optical slices through the middle of seeds. In the wild type (WT), 2F4 labels attached primary walls (arrowheads). For *fly1-1*, 2F4 labels both the detached primary walls (arrows) and the underlying mucilage. Bars = 50 μm.

(F) Biochemical determination of pectin DM in mucilage and whole seeds. Wild-type and *fly1-1* whole seeds have a similar DM, but *fly1-1* mucilage has a significantly lower DM than wild-type mucilage. Values represent the mean ± SE of four technical replicates. Two additional biological replicates showed the same trend.

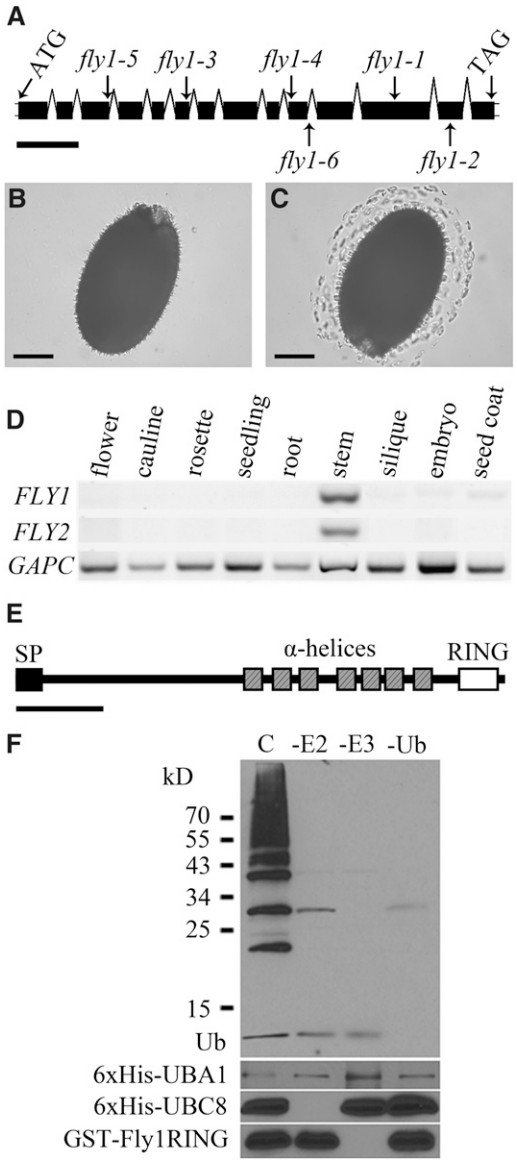

Figure 5. Characterization of the *FLY1* Gene and Its Encoded Protein.

(A) *FLY1* gene structure and mutations. T-DNA insertions (*fly1-2* to *fly1-6*) are indicated with arrows. Boxes and connecting lines represent exons and introns.

(B) and **(C)** Genomic complementation of *fly1-1* with At4g28370.

(B) *fly1-1* plants transformed with $FLY1_{pro}$:*FLY1-YFP* produce seeds that do not release discs.

(C) *fly1-1* plants transformed with an empty pGreenII0229 vector produced seeds that still released discs.

(D) RT-PCR analysis of *FLY1* and *FLY2* transcripts in Col-2 tissues. Embryo and seed coat RNA was isolated from seeds at 7 DPA. *GAPC* was used as a loading control.

(E) Predicted architecture of the FLY1 protein. FLY1 has a signal peptide (SP), seven α-helices (Schwacke et al., 2003), and a RING-H2 domain. Bars = 300 bp in **(A)**, 150 μm in **(B)** and **(C)**, and 100 amino acids in **(E)**.

(F) The FLY1 RING domain has E3 ubiquitin ligase activity in vitro. Complete (C) ubiquitination assays contained E1 enzyme 6xHis-At-UBA1, E2 enzyme 6xHis-At-UBC8, E3 enzyme GST-Fly1RING (only includes the soluble RING domain), and Ubiquitin (Ub). Top: Immunoblot using anti-Ub. The ladder and smear represent poly-Ub species of the enzymes present in the reaction. No poly-Ub is detected when omitting 6xHis-At-UBC8 (-E2 lane), GST-Fly1RING (-E3 lane), or ubiquitin (-Ub lane) from the assay. The asterisk marks
anti-Ub cross-reacting with the E3 enzyme. Center: anti-His to detect E1 and E2 enzymes. Bottom: anti-GST to detect GST-Fly1RING.

database (Mutwil et al., 2008), *FLY1* and *FLY2* are highly coexpressed with *KNOTTED1-LIKE HOMEODOMAIN PROTEIN7* (*KNAT7*), which encodes a transcription factor shown to regulate cell wall biosynthesis in xylem and seed coat cells (Romano et al., 2012; Bhargava et al., 2013). Although *knat7* mutants display an irregular xylem cell phenotype, both *fly1* and *fly2* xylem cells resembled the wild type (see Supplemental Figure 8B online).

Analysis of the FLY1 Peptide Sequence

FLY1 contains an N-terminal signal peptide that targets the protein to the endomembrane system (Petersen et al., 2011) and is predicted to be cleaved in the endoplasmic reticulum between amino acids 32 and 33. The consensus prediction of the ARAMEMNON plant membrane protein database is that FLY1 has seven transmembrane-spanning α-helices (Figure 5E; Schwacke et al., 2003). The C-terminal end of the FLY1 protein contains a RING finger, which is conserved in all eukaryotes and coordinates two zinc ions (Quevillon et al., 2005; Sigrist et al., 2010; Lamesch et al., 2012). The predicted ARAMEMNON topology of the FLY1 protein indicates that the C-terminal RING domain faces the cytosol. Both FLY1 and FLY2 have a RING domain with a C3H2C3 motif (abbreviated RING-H2; Stone et al., 2005) based on the arrangement of the eight zinc binding Cys and His residues (see Supplemental Figure 9 online). Interestingly, the ortholog of FLY1 (28% amino acid identity) in the yeast *Saccharomyces cerevisiae* is TRANSMEMBRANE UBIQUITIN LIGASE1 (TUL1), a Golgi-localized E3 ligase that tags misfolded membrane proteins with ubiquitin for transport to endosomes and degradation in the vacuole (Reggiori and Pelham, 2002). TUL1 has a C-terminal RING-H2 domain similar to FLY1 and FLY2 (see Supplemental Figure 9 online), along with an N-terminal signal peptide and seven α-helices (Reggiori and Pelham, 2002).

To determine if FLY1 functions as an E3 ligase, we conducted an in vitro ubiquitination assay (Hardtke et al., 2002). Ubiquitination results from the sequential action of a ubiquitin-activating enzyme (E1), a ubiquitin-conjugating enzyme (E2), and a ubiquitin ligase (E3) and can regulate a protein's stability, activity, or location (Hicke and Dunn, 2003; MacGurn et al., 2012). Since recombinant expression and purification of transmembrane proteins is challenging, we expressed only the soluble C terminus of FLY1 containing the RING domain fused to glutathione *S*-transferase (GST-Fly1RING). The complete in vitro ubiquitination assay contained ubiquitin and three recombinant *Arabidopsis* proteins: E1 enzyme 6xHis-UBA1, E2 enzyme 6xHis-UBC8, and E3 enzyme GST-Fly1RING. The polyubiquitin smear, detected by immunoblot analysis using an antiubiquitin antibody in the complete assay (Figure 5F), demonstrates that the FLY1 RING

domain is capable of mediating polyubiquitination. Omission of the E2 enzyme, the E3 ligase, or the ubiquitin components abolished formation of polyubiquitinated species as expected (Figure 5F).

The E3 ubiquitin ligase activity of FLY1 and the lower pectin DM of *fly1* mucilage suggest that FLY1 may positively regulate PMTs or negatively regulate PMEs. While putative PMTs are membrane bound (Mouille et al., 2007, Held et al., 2011; Miao et al., 2011), most PMEs are soluble or have a signal peptide that is cleaved in the endoplasmic reticulum (Pelloux et al., 2007) and therefore do not have cytosolic Lys residues, which can be ubiquitinated (MacGurn et al., 2012). Thus, we investigated if PMEs coexpressed with FLY1 have membrane domains and putative ubiquitination sites. *PME6* (At1g23200) and *PME16* (At2g43050) are preferentially expressed in the seed coat and are coexpressed with FLY1 in GeneCAT (Mutwil et al., 2008) and ATTED-II databases (Obayashi et al., 2011). Unlike most PMEs, PME6 and PME16 are predicted to have an internal α-helix near the N terminus and at least one cytosolic Lys residue (Schwacke et al., 2003).

FLY1-YFP Expression and Subcellular Localization

The expression and subcellular localization of FLY1 was analyzed using the previously described *FLY1*$_{pro}$:*FLY1-YFP* construct that complements the *fly1-1* mutation (Figure 5B). We used identical image acquisition settings for the different tissues and developmental stages presented within each figure. Multiple independent plants containing the *FLY1*$_{pro}$:*FLY1-YFP* transgene displayed strong YFP fluorescence in the seed coat epidermis (Figure 6; see Supplemental Figure 10 online). FLY1-YFP expression begins at 4 DPA, is highest at 7 DPA, when mucilage synthesis and secretion is at its peak, and decreases by 10 DPA, at the start of columella deposition (see Supplemental Figures 10A to 10F online). No FLY1-YFP signal was observed in dissected embryos at 7 DPA (see Supplemental Figure 10H online) or in tissues more suitable for cell imaging such as leaves and roots.

FLY1-YFP fusion proteins primarily localize in a small number of intracellular punctae in seed coat epidermal cells and are not observed in the mucilage pocket or in the primary cell wall (Figure 6). At 7 DPA, FLY1-YFP fluorescence also appears in several larger compartments (Figures 6D and 6J, arrows). Since TUL1 is known to be Golgi localized (Reggiori and Pelham, 2002), we compared the localization of FLY1-YFP with the distribution of the Golgi marker α-2,6-sialyltransferase (ST) tagged with red fluorescent protein (RFP; Batoko et al., 2000; Brandizzi et al., 2002; Lee et al., 2002). ST-RFP labels a large number of intracellular punctae (Figures 6B and 6E), which are in close proximity to FLY1-YFP bodies and partially overlap with a few of them (Figures 6A to 6F, arrowheads). Surprisingly, however, the majority of FLY1-YFP compartments do not colocalize with the Golgi marker ST-RFP at either 4 or 7 DPA (Figures 6C and 6F). We also analyzed the subcellular localization of the *trans*-Golgi network/early endosome (TGN/EE) marker VHAa1-RFP (Dettmer et al., 2006), which is distinct from the Golgi marker ST-RFP (Viotti et al., 2010). Although a few FLY1-YFP punctae partially colocalize with VHAa1-RFP in seed coat epidermal cells at 4 and 7 DPA (Figures 6G to 6L, arrowheads), the localization of FLY1-YFP is largely distinct from that of the TGN/EE. The fluorescent markers tested were excluded from seed coat mucilage pockets and the amyloplasts (Figure 6).

We were unable to stain seeds expressing FLY1-YFP with the endocytic tracer FM4-64 (Viotti et al., 2010) due to a lack of dye uptake by developing seed coat cells. Seed epidermal cells pretreated with 10% DMSO to increase permeability were also not affected by Brefeldin A, a drug commonly used in secretion and endocytosis studies (Robinson et al., 2008). However, 7 DPA seed coat epidermal cells treated with wortmannin, a drug that induces the fusion of late endosomes/multivesicular bodies/prevacuolar compartments (LEs/MVBs/PVCs) in plants (Wang et al., 2009), showed a greater number of large FLY1-YFP bodies than control seeds (see Supplemental Figures 11A and 11B online). Wortmannin treatment increased the ratio of large to small FLY1-YFP bodies from 2 to 39% in one biological replicate and from 13 to 28% in a second biological replicate (see Supplemental Figures 11C and 11D online).

DISCUSSION

We identified the *FLY1* locus through a forward genetic screen for *Arabidopsis* mutants with abnormal seed mucilage extrusion. Histological and biochemical analyses revealed that loss-of-function mutations in the *FLY1* gene cause two distinct mucilage defects when seeds are hydrated in water. The most obvious phenotype of *fly1* mutant seeds is the presence of a large number of disc-like structures at the edge of the extruded mucilage capsule. The discs appear to be mucilage-bound primary cell walls that detach from the columellae of epidermal cells. Close examination of *fly1* seeds revealed that mucilage extrusion is also impaired, resulting in a more compact RR-stained capsule that is more difficult to extract than wild-type mucilage. Despite these defects, *fly1* and wild-type seeds produce similar amounts of mucilage and display indistinguishable morphology during development. We found that hydration of *fly1* seeds in a $CaCl_2$ solution significantly impairs mucilage release, suggesting that *fly1* mucilage can form more pectin cross-links mediated by Ca^{2+} ions than the wild type. Calcium bridges are required to cross-link unesterified HG chains and to maintain the strength of pectin gels (Willats et al., 2001a). EDTA, a cation chelator, completely rescues the *fly1* mutant phenotype at pH 8.0, including both the size of the mucilage capsule and the disc formation. Alkaline solutions can degrade pectin gels (Sriamornsak, 2003), but a HEPES pH 8.0 treatment, which does not remove Ca^{2+} ions, only partially rescued the mutant phenotype. All *fly1* seed epidermal cells treated with EDTA pH 8.0 surprisingly had outer tangential primary walls attached to their columellae and no visible discs, suggesting that *fly1* primary wall detachment does not result from weaker connections to the columellae. Instead, the force generated by slowly expanding mucilage may detach the primary walls from columellae of *fly1* seeds hydrated in water. Therefore, the primary defect in *fly1* appears to be increased mucilage cohesion.

Since HG with a low DM represents the only cell wall component that uses Ca^{2+} ions as its main mechanism for cross-linking, *fly1* mucilage was expected to contain more unesterified

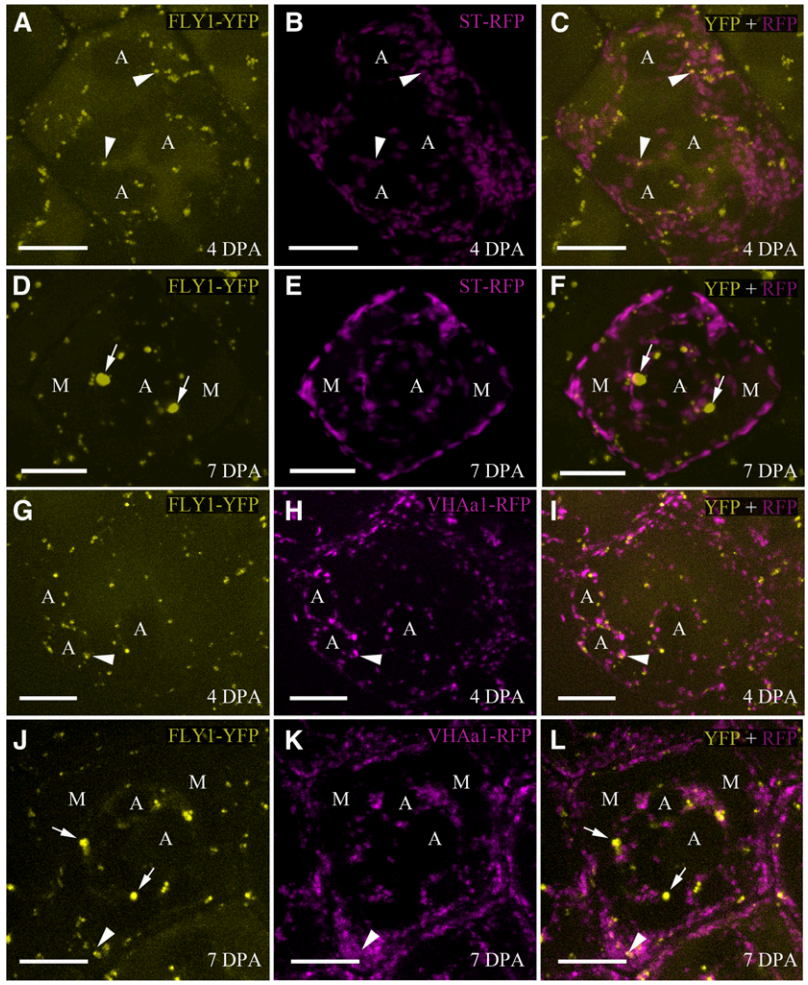

Figure 6. Localization of FLY1-YFP, ST-RFP, and VHAa1-RFP in Seed Coat Epidermal Cells.

Maximum intensity signals from multiple stacks. Composite images (right panels) of FLY1-YFP (left panels) and RFP-tagged markers (middle panels). FLY1-YFP is localized in punctae at 4 DPA (**[A]** and **[G]**) and in punctae and larger bodies (arrows) at 7 DPA (**[D]** and **[J]**). FLY1-YFP punctae are associated with (arrowheads) but predominantly distinct from the Golgi marker ST-RFP (**[C]** and **[F]**) and the TGN/EE marker VHAa1-RFP (**[I]** and **[L]**). A, amyloplasts. M, mucilage pockets. Bars = 10 μm.

HG than the wild type. Indeed, seed immunolabeling with three anti-HG antibodies and biochemical assays of the pectin DM demonstrate that *fly1* mucilage has a significantly lower DM than wild-type mucilage. An increased number of unesterified HG blocks would strengthen the pectin gel matrix, reduce mucilage expansion, and increase its adherence to the seed, consistent with the *fly1* mucilage defects. Increased binding of mucilage to the primary wall combined with reduced extrusion may generate sufficient pressure for mucilage to detach outer primary walls from columellae when *fly1* is hydrated in water. The 2F4 immunolabeling supports this model, as unesterified HG was detected in both the *fly1* discs and the underlying compact mucilage columns. Although mucilage is mainly composed of unbranched RG-I (Western et al., 2000, 2004; Penfield et al., 2001; Usadel et al., 2004; Dean et al., 2007; Macquet et al., 2007a, 2007b), changes in the DM of HG can have a profound impact on the entire pectin gel matrix if RG-I and HG are covalently bonded as the current models suggest (Harholt et al., 2010). Overall, the analysis of *fly1* seeds suggests that *FLY1* is required for maintaining a high pectin DM in seed mucilage.

We identified *FLY1* as At4g28370 using positional cloning and showed that multiple independent T-DNA alleles have the same phenotype as the *fly1-1* EMS line. Molecular complementation of *fly1-1* with a $FLY1_{pro}$:*FLY1-YFP* transgene rescued the mutant phenotype. The *FLY1* gene encodes a previously uncharacterized protein with seven transmembrane spans and a C-terminal RING-H2 domain. RING fingers are the catalytic sites of E3 ubiquitin ligases, which mediate the transfer of ubiquitin from an E2 ubiquitin-conjugating enzyme to target proteins (Glickman and Ciechanover, 2002). Since FLY1 and FLY2 are putative E3 ligases (Stone et al., 2005) and their yeast ortholog, TUL1, is a known yeast E3 ligase (Reggiori and Pelham, 2002), we tested the ability of the FLY1 RING-H2 domain to transfer ubiquitin to a substrate in vitro (Hardtke et al., 2002). As predicted in silico,

the FLY1 RING domain functions as an E3 ligase in the in vitro ubiquitination assay.

We investigated the expression and subcellular localization of FLY1-YFP under the transcriptional control of the native FLY1 promoter. FLY1-YFP displayed a punctate distribution in the cytoplasm of developing seed coat epidermal cells but also appeared in enlarged bodies at the stage of mucilage biosynthesis. Unlike TUL1, which is Golgi localized (Reggiori and Pelham, 2002), the majority of FLY1-YFP compartments were distinct from the Golgi marker ST-RFP in seed coat epidermal cells. We also found that, despite occasional overlap, the majority of FLY1-YFP punctae did not colocalize with the TGN/EE marker VHAa1-RFP. In addition, FLY1-YFP does not resemble the reticular distribution of endoplasmic reticulum or the linear distribution of plasma membrane (PM) markers. Thus, FLY1-YFP most likely resides in a compartment between the TGN/EE and the PM, namely, the LE/MVB/PVC and/or the vacuole (Müller et al., 2007). Although FM4-64 and Brefeldin A were not taken up by seed coat epidermal cells, we successfully treated seeds with wortmannin, which induces the fusion of LE/MVB/PVC in plant cells (Wang et al., 2009). Consistent with FLY1-YFP being localized in LE/MVB/PVC, wortmannin-treated seeds displayed fewer punctae and an increased number of large bodies.

A remaining question concerns the manner in which FLY1, a transmembrane E3 ligase that appears to be associated with the post-Golgi endomembrane system, can influence the level of DM in mucilage. Pectin DM is controlled by the activity of PMTs that add methylester groups and PMEs that remove methylester groups (Wolf et al., 2009a). Since *fly1* mucilage has a lower DM relative to the wild type, FLY1 could be promoting PMT activity or decreasing PME activity.

As an E3 ligase, FLY1 could mark PMTs with monoubiquitin for retention in the Golgi since monoubiquitin has been identified as a signal for membrane protein localization in yeast, animal, and plant systems (Reggiori and Pelham, 2002; Hicke and Dunn, 2003; Schnell and Hicke, 2003, Barberon et al., 2011; Dowil et al., 2011). Alternatively, the FLY1 E3 ligase could use polyubiquitin chains to target PME proteins for degradation.

Although PMTs are predicted to have a single membrane-spanning domain (Krupková et al., 2007), this may not be sufficient for Golgi localization as the mechanisms for the retention of plant proteins in the Golgi are not well understood (Saint-Jore-Dupas et al., 2004). None of the 67 putative PMTs in the *Arabidopsis* genome have a confirmed biochemical activity (Harholt et al., 2010), and only a few, such as QUA2 (Mouille et al., 2007), QUA3 (Miao et al., 2011), and CGR3 (Held et al., 2011), are known to impact pectin biosynthesis. Because the putative PMTs studied to date are Golgi localized and FLY1-YFP localization appeared distinct from the Golgi marker ST-RFP, we do not favor the hypothesis that FLY1 targets PMTs.

A second possibility for the role of FLY1 in controlling pectin DM is that FLY1 is needed to recycle PMEs active in seed mucilage. Recycling of PME enzymes by FLY1 in wild-type cells may be essential for establishing the correct level of pectin DM in the mucilage pockets to facilitate proper mucilage extrusion.

PMEs are typically soluble (Pelloux et al., 2007) and lack the cytosolic Lys residues required for ubiquitination, but there are at least two PMEs that are preferentially expressed in the seed coat and have putative ubiquitination sites. Both PME6 and PME16 are classified as Type I/Group 2 PMEs because they also contain a PRO region with PME inhibitor homology and a processing motif for cleavage by subtilisin-like proteases (Pelloux et al., 2007; Wolf et al., 2009b). While PMEs whose PRO region is not cleaved are predicted to be retained in the Golgi (Wolf et al., 2009b), recent data suggest that certain Type I/Group 2 PMEs can be secreted to the cell wall without processing (Mareck et al., 2012). Therefore, FLY1 could be recycling unprocessed PMEs post-Golgi or upon endocytosis from the PM. Interestingly, elevated PME activity during seed coat development was proposed to cause reduced mucilage extrusion and primary wall detachment in the *sbt1.7* (Rautengarten et al., 2008) and *pmei6* (Saez-Aguayo et al., 2013) mutants. However, unlike *fly1* discs, *sbt1.7* and *pmei6* outer tangential primary walls detach as a large continuous sheet (Rautengarten et al., 2008; Saez-Aguayo et al., 2013), suggesting that FLY1 functions independently of SBT1.7 and PMEI6.

The identification of FLY1, a transmembrane E3 ubiquitin ligase that controls the pectin DM in seed mucilage and is required for proper seed mucilage extrusion, is an important step forward in unraveling how plant cells synthesize, secrete, and modify pectin polymers. Detailed characterization of the *fly1* seed coat phenotype revealed an unexpected scenario where primary cell wall detachment appears to result from the extrusion of mucilage with stronger gelling properties and an increased number of HG cross-links via calcium bridges. The discovery of the targets of the FLY1 protein and the elucidation of role of ubiquitination in the regulation of pectin DM may provide new perspectives on pectin modification and on the regulation of cell wall enzymes in the endomembrane system. This protein also offers a great opportunity to identify components of the pectin methylesterification pathway that are active in *Arabidopsis* seed mucilage. Finally, since *FLY1* and *FLY2* are both expressed in the xylem, it will be of interest to examine the development of this tissue in *fly1 fly2* double mutants.

METHODS

Plant Materials and Growth Conditions

The Col-2 ecotype was propagated from a Columbia-0 (Col-0) seed through five generations of single seed descent by Shauna Somerville. The *fly1-1* line was isolated from an EMS-mutagenized Col-2 population and was backcrossed to Col-2 four times to remove background EMS mutations. The *fly1-1* mutant line (backcrossed twice to Col-2) was crossed to the Landsberg *erecta* (L*er*) ecotype to generate an F2 mapping population. Map-based cloning was conducted using insertion/deletion polymorphisms between Col-0 and Landsberg *erecta* (Jander et al., 2002). Col-0 seeds bearing SALK T-DNA insertions in exons (Alonso et al., 2003), 5′ untranslated regions (UTRs), or introns (in decreasing order of preference) were selected using the SIGnAL T-DNA Express site (http://signal.salk.edu/cgi-bin/tdnaexpress) and obtained from the ABRC in Columbus, Ohio.

Seeds were germinated on plates with AT medium (Haughn and Somerville, 1986) and 7% (w/v) agar, and seedlings were transferred to soil (Sunshine Mix 4; SunGro) after 7 to 10 d. Plants were grown with continuous fluorescent illumination of 80 to 140 μE m^{-2} s^{-1} at 20 to 22°C. Developing seeds were staged as previously described (Western et al., 2001).

Preparation of Seed Coat Sections

Developing seeds were fixed using high-pressure freezing and freeze substitution, embedded in Spurr's resin, and sectioned according to

previous methods (Rensing et al., 2002; Young et al., 2008; Mendu et al., 2011). Well-preserved seed coats were examined by light microscopy.

Light Microscopy

Mature dry seeds were hydrated in distilled water, 50 mM $CaCl_2$, or 50mM EDTA, pH 8.0, for 1 to 2 h, rinsed with once with water, and stained with 0.01% (w/v) RR (Sigma-Aldrich) for 30 to 60 min while shaking on a rotator. Bright-field micrographs of stained samples were taken with QCapture software and a digital camera (QImaging) equipped on a Zeiss AxioSkop 2 upright light microscope (Carl Zeiss). Contrast of unstained seeds was enhanced with phase contrast or differential interference contrast.

The effect of buffer pH on *fly1-1* mucilage extrusion was tested using 50 mM EDTA and 50 mM HEPES buffers ranging from pH 6.0 to 8.0. Seeds were shaken in buffer for 1 h before rinsing with water and RR staining.

Live, developing seeds at 12 DPA were imaged using transmitted light on a Perkin-Elmer Ultraview VoX Spinning Disk Confocal system.

For cellulose staining, seeds were shaken in water for 2 h and then mixed with 0.01% (w/v) S4B (Sigma-Aldrich Rare Chemical Library) and 50 to 150 mM NaCl for 1 h (Anderson et al., 2010; Mendu et al., 2011). Seeds were rinsed twice with distilled water and imaged using a 561-nm laser on either a Zeiss 510 Meta laser scanning confocal microscope (Carl Zeiss) or a Perkin-Elmer Ultraview VoX spinning disk confocal system. Xylem cells were analyzed in stem base cross sections stained with one drop of saturated phloroglucinol (Sigma-Aldrich) in 20% HCl solution.

Immunohistochemistry

Whole-seed immunolabeling was conducted according to a published method (Harpaz-Saad et al., 2011). The specificities of JIM5, JIM7 (CarboSource), and 2F4 (PlantProbes) primary antibodies have been extensively described (Liners et al., 1989; Knox et al., 1990; Knox, 1997; Willats et al., 2001b; Macquet et al., 2007a; Pattathil et al., 2010; Xu et al., 2011). The 2F4 antibody (PlantProbes) does not work with the conventional phosphate buffer (Liners et al., 1989) and was used with the following buffer: 20 mM Tris-HCl, pH 8.2, 0.5 mM $CaCl_2$, and 150 mM NaCl. Goat-anti-rat secondary antibody conjugated to AlexaFluor488 was used against JIM5 and JIM7, while goat-anti-mouse conjugated to AlexaFluor488 (Molecular Probes, Invitrogen) was used against 2F4. The protocol was performed without primary antibody as a negative control. Seeds were imaged using a 488-nm laser (antibody fluorescence) and 561-nm laser (seed intrinsic fluorescence, background) on a Zeiss 510 Meta laser scanning confocal microscope (Carl Zeiss) or a Perkin-Elmer Ultraview VoX spinning disk confocal system. All confocal micrographs were processed with ImageJ (Abramoff et al., 2004). Images containing signals from multiple optical stacks were rendered using the Z-project maximum intensity method.

Scanning Electron Microscopy

Dry seeds were mounted on stubs, coated with gold-palladium in a SEMPrep2 sputter coater (Nanotech), and examined with a Hitachi S4700 scanning electron microscope (Hitachi High-Technologies). For cryo-scanning electron microscopy, seeds were hydrated with a drop of distilled water and were quickly transferred to stubs topped with Tissue-Tek mounting medium (Sakura Finetek) and small squares of filter paper to absorb excess water. Once mounted on the stubs, seeds were immediately frozen in liquid nitrogen. Samples were analyzed under high vacuum at liquid nitrogen temperatures with a Hitachi S-4700 field emission scanning electron microscope (Hitachi High-Technologies) equipped with a Leica VCT 100 cryo transfer system and cryo stage control (Leica).

Light and electron micrographs were processed and measured with ImageJ (Abramoff et al., 2004). Image panels were made using Photoshop (Adobe Systems).

Determination of Monosaccharide Composition by HPAEC

The average weight of Col-2 and *fly1-1* seeds was determined by weighing three replicates of 100 seeds for each genotype. For sequential mucilage extractions, four technical replicates of 25 mg of Col-2 or *fly1-1* seeds (exact weight recorded) were mixed with 1.4 mL of distilled water and 10 μL of 5 mg/mL D-erythritol (internal standard). These samples were gently shaken using a tube rotator for 1 h. The mucilage in the supernatant (1 mL) of the first extraction was transferred to a glass tube and dried at 60°C under nitrogen gas. The same seeds were then rinsed twice with 700 μL of water and shaken vigorously with a vortex mixer on the highest setting for 2 h, in 1.4 mL of water and 10 μL of 5 mg/mL D-erythritol. The supernatant was transferred to a new glass tube and dried as described for the first extraction. Whole seeds, sugar standards dissolved in water, and the dried mucilage samples were processed according to published methods (Dean et al., 2007; Mendu et al., 2011).

Biochemical Determination of Pectin DM

Mucilage was extracted by vigorously shaking 5 mg of seeds (exact weight measured) with a vortex mixer at high speed in 300 μL of 50 mM EDTA for 60 min. After the seeds settled for 2 min, 100 μL of supernatant was transferred to a new tube and saponified with 0.25 M NaOH for 60 min on an orbital shaker. The reaction was neutralized with 0.25 M HCl (to give a total volume of 300 μL) and centrifuged for 5 min at 10,000*g*. Fifty microliters of the supernatant was transferred to a 96-well plate for the methanol release after saponification assay (Lionetti et al., 2007), using 0.5 units of alcohol oxidase (Sigma-Aldrich A2404) enzyme per sample instead of 0.03 units. Absorbance was measured at 412 nm and quantified using a methanol standard curve (Klavons and Bennett, 1986).

Forty microliters of the remaining 250 μL mucilage saponification solution was transferred to a 96-well plate, and the uronic acid assay was performed as described by van den Hoogen et al. (1998). Absorbance was measured at 525 nm, before and after addition of the dye, and quantified using a D-(+)-galacturonic acid monohydrate (Sigma-Aldrich) standard curve.

For whole seed analysis, 5 mg of seeds were frozen in liquid nitrogen and ground to a find powder using pestles in 1.7-mL tubes. Ground seeds were washed twice with 500 μL of 70% ethanol on an orbital shaker and centrifuged for 2 min at 10,000*g*. Ethanol was removed again and the pellet was dried under nitrogen gas at 60°C. One additional methanol-chloroform (1:1) wash and three acetone washes were performed under similar conditions. After the final wash, samples were dried under nitrogen gas at 60°C and the cell wall pellet was saponified using 200 μL of 0.25 M NaOH for 60 min on an orbital shaker. Samples were neutralized with 200 μL of 0.25 M HCl and centrifuged for 5 min at 10,000*g*. Fifty microliters of the supernatant was used for the 96-well plate methanol assay (Lionetti et al., 2007). Background corrections for methanol assay were made using mucilage and whole seed samples that were not saponified.

The whole seed sugars in the leftover saponification reaction were precipitated by adding 1 mL of 100% ethanol, vortexing briefly, and centrifuging for 2 min at 10,000*g*. The supernatant was removed and the cell wall pellet was dried under nitrogen gas at 60°C. The cell wall was fully resuspended in 1 mL distilled water. Each sample was sonicated for 20 s with a Branson Sonifier 150 (Branson Ultrasonics), setting 3, to create a homogenous cell wall suspension. Twenty-microliter aliquots of each sample, diluted with 20 μL water, were used for the 96-well plate uronic acid assay (van den Hoogen et al., 1998).

DNA Isolation and T-DNA Genotyping

DNA was isolated from rosette leaves using a published one-step protocol (Kasajima et al., 2004), except that samples were quickly ground using 1.0-mm zirconia/silica beads (Biospec Products) and a Precellys 24 tissue homogenizer (Bertin Technologies) (Verollet, 2008) instead of homogenization using plastic pestles. The supernatant was used immediately (1 μL of DNA solution in 20 μL PCR reaction) or was stored at −20°C until needed.

SALK T-DNA insertions were genotyped by PCR using the LBb1.3 insert-specific primer (5′-ATTTTGCCGATTTCGGAAC-3′) and gene-specific primers selected using the SALK T-DNA Primer Design tool (http://signal.salk.edu/tdnaprimers.2.html; see Supplemental Table 1 online).

Protein Bioinformatics

All genes in this study were first analyzed using The Arabidopsis Information Resource (http://Arabidopsis.org; Lamesch et al., 2012). The SignalP 4.0 server (http://www.cbs.dtu.dk/services/SignalP) was used for signal peptide analysis (Petersen et al., 2011). Transmembrane α-helices were predicted using the ARAMEMNON database (http://aramemnon.botanik.uni-koeln.de), which integrates the predictions of 18 individual programs (Schwacke et al., 2003). *FLY1* homologs identified using BLAST programs (http://blast.ncbi.nlm.nih.gov/Blast.cgi) were verified using the Phytozome (http://www.phytozome.net; Goodstein et al., 2012), PLAZA (http://bioinformatics.psb.ugent.be/plaza; Van Bel et al., 2012), and the InParanoid 7 databases (http://InParanoid.sbc.su.se; Ostlund et al., 2010).

Functional domains were identified using the InterProScan (http://www.ebi.ac.uk/Tools/pfa/iprscan; Quevillon et al., 2005) and PROSITE databases (http://prosite.expasy.org; Sigrist et al., 2010). FLY1, FLY2, and TUL1 protein sequences were aligned using ClustalW2 (http://www.ebi.ac.uk/Tools/msa/clustalw2; Larkin et al., 2007).

Recombinant Protein Expression and Purification

The soluble C-terminal FLY1 region (after the seventh transmembrane domain and before the stop codon) containing the RING domain was amplified using a left primer (LP) plus *Eco*RI site (5′-tgaGAATTCCTCACGCTGCTTTGTTCCCCGTCAGA-3′) and a right primer (RP) plus *Xho*I site (5′-tatCTCGAGCTATGCTGGAGGAAGAGACCGCCGA-3′) using Col-2 seed coat cDNA. The resulting 243-bp Fly1RING amplicon was fused with GST using an *Eco*RI-*Xho*I cassette on the pGEX-4T-3 vector (GE Healthcare). The plasmid was propagated in *Escherichia coli* DH5α cells, verified by sequencing, and transformed in *E. coli* BL21(DE3)-pLysS for protein expression. A 50 mL culture was grown until OD_{600} = 0.5, when it was induced with 0.5 mM Isopropyl β-D-1-thiogalactopyranoside (IPTG) and grown for additional 4 h. Cells were harvested by centrifugation and resuspended in 2 mL lysis buffer (25 mM Tris-HCl, pH 7.5, 500 mM NaCl, 0.01% [v/v] Triton-X, and one protease inhibitor tablet [Roche]) and sonicated three times at 20% amplitude and 20 mA for 30 s. Lysate was cleared by centrifugation at 12,000*g* for 15 min at 4°C followed by filtration through a 0.45 mM filter. For purification, 200 μL of 50% glutathione agarose slurry (Sigma-Aldrich) was added to the cleared lysate and incubated under rotation at 4°C for 2 h. Sample was washed four times with 1 mL wash buffer (25 mM Tris-HCl, pH 7.5, 300 mM NaCl, and 0.01% [v/v] Triton-X) and purified protein eluted in 100 mL elution buffer (25 mM Tris-HCl, pH 7.5, 150 mM NaCl, 0.01% [v/v] Triton-X, and 15 mM reduced glutathione); glycerol was added to a final concentration of 40% (v/v).

The 6xHis-UBC8 and 6xHis-UBA1 *Arabidopsis thaliana* recombinant proteins were expressed in *E. coli* BL21-AI (Invitrogen) and induced with 0.2% (w/v) arabinose at an OD_{600} = 0.5. Proteins were purified on a nickel-nitrilotriacetic acid (Ni-NTA) column according to the manufacturer's instructions (Qiagen) with lysis buffer (50 mM NaH_2PO_4, pH 8.0, 300 mM NaCl, and 10 mM imidazole). In wash buffer, the concentration of imidazole was increased to 20 mM and the elution buffer contained 250 mM imidazole.

Protein purity was analyzed by SDS-PAGE followed by Coomassie Brilliant Blue staining, and concentration was measured by Bradford assay (Bio-Rad). The integrity of fusion proteins was checked by immunoblot analysis using anti-GST and anti-His antibodies (both Sigma-Aldrich).

In Vitro Ubiquitination Assay

In vitro ubiquitination assays were performed as previously described in Hardtke et al. (2002). In 30-μL reactions (50 mM Tris-HCl, pH 7.5, 10 mM $MgCl_2$, 1 mM ATP, 0.05 mM $ZnCl_2$, 0.2 mM DTT, 10 mM phosphocreatine, 0.1 units of phosphocreatine kinase), 100 ng E1 (6xHis-UBA1), 250 ng E2 (6xHis-UBC8), 2 μg ubiquitin (BostonBiochem), and 250 ng GST-Fly1RING were added for the complete reaction. For control reactions, the E2, E3, or ubiquitin components were omitted. The reactions were incubated at 30°C for 2 h and stopped by addition of 3.3 μL 10× reducing loading buffer. Samples were separated by SDS-PAGE, blotted onto nitrocellulose membranes, and probed with anti-ubiquitin (Enzo Life Sciences).

Transcript Analysis

Expression patterns in specific *Arabidopsis* organs and cell types were visualized with the eFP browser (http://bar.utoronto.ca/efp/cgi-bin/efpWeb.cgi; Winter et al., 2007) and corroborated with GENEVESTIGATOR (https://www.genevestigator.com/gv/plant.jsp; Hruz et al., 2008).

For RT-PCR, RNA was extracted from Col-2 tissues using the RNeasy mini kit (Qiagen) according to the manufacturer's instructions. RNA quantification was performed using a NanoDrop 8000 (Thermo Scientific). Five hundred nanograms of total RNA treated with DNaseI (Fermentas) was used for first-strand cDNA synthesis along with iScript RT supermix (Bio-Rad). RT-PCR was conducted using a typical PCR reaction containing Taq polymerase (Invitrogen) and gene-specific pairs of intron-spanning primers (see Supplemental Table 1 online). Amplicons of ~200 bp were expected after intron splicing. Transcript levels were analyzed after 23 amplification cycles, and *GAPC* was used as a loading control.

$FLY1_{pro}$:FLY1-YFP Cloning

FLY1 was amplified from Col-2 DNA using Phusion High-Fidelity DNA polymerase (Thermo Fisher Scientific), an LP plus a *Kpn*I site (5′-gcgGGTACCtctcacaaacaaacatttctcactc-3′) and an RP including an *Xho*I site (5′-tactcgagTGCTGGAGGAAGAGACCGCCGACAA-3′). The 5156-bp $FLY1_{pro}$:*FLY1* amplicon starts 690 bp upstream of the 5′ UTR of *FLY1* (123 bp away from the At4g28365 5′ UTR, its upstream neighbor) and includes the complete *FLY1* coding region, except for the translation stop codon.

Citrine YFP was selected due to its superior photostability in the acidic environment of the apoplast. The $FLY1_{pro}$:*FLY* amplicon was introduced as a *Kpn*I-*Xho*I cassette into a pAD vector with Citrine YFP (DeBono, 2012). The plasmid was propagated in *E. coli* DH5α cells and verified using *Bgl*II restriction enzyme digestion and sequencing. The $FLY1_{pro}$:*FLY-YFP* construct was introduced in *Arabidopsis fly1-1* plants by the floral dip method (Clough and Bent, 1998) using *Agrobacterium tumefaciens* GV3101 pMP90 plus pSOUP (Hellens et al., 2000).

FLY1-YFP, ST-RFP, and VHAa1-RFP Subcellular Localization

Transgenic plants were selected by spraying the leaves of plants germinated on soil with 200 mM Basta herbicide solution every 2 to 3 d for 2 weeks. Seeds were removed from developing siliques of Basta-resistant transgenic plants. FLY1-YFP and ST-RFP/VHAa1-RFP were excited

using 514- and 561-nm lasers, respectively, on a Perkin-Elmer Ultraview VoX spinning disk confocal system. FLY1-YFP expression in dissected seed coats, embryos, and other tissues was examined with a ×20 oil immersion objective, while subcellular localization of the FLY1-YFP signal was investigated with a ×63 glycerol immersion objective. The controls used were untransformed Col-2 and *fly1-1* seeds and transgenic lines expressing a single fluorescent construct. In addition, 7 DPA seeds expressing *FLY1*$_{pro}$*:FLY-YFP* were dissected from siliques and treated for 2 h with 20 μM wortmannin (diluted in water from a 1 mM DMSO stock) or with water containing an equivalent amount of DMSO, before imaging.

Accession Numbers

Sequence data from this article can be found in the Arabidopsis Genome Initiative or GenBank/EMBL databases under accession numbers At4g28370 (*FLY1*) and At2g20650 (*FLY2*).

Supplemental Data

The following materials are available in the online version of this article.

Supplemental Figure 1. Analysis of *fly1-1* Mucilage Extrusion and Primary Wall Attachment.

Supplemental Figure 2. Mucilage Extractions and Total Monosaccharide Composition.

Supplemental Figure 3. Time-Course Analysis of Mucilage Release from Seeds upon Hydration.

Supplemental Figure 4. Analysis of the Effect of Buffer pH on *fly1-1* Mucilage Defects.

Supplemental Figure 5. Immunolabeling of Partially Methylesterified HG in Seeds.

Supplemental Figure 6. Analysis of *fly1* and *fly2* Mucilage Extrusion.

Supplemental Figure 7. *FLY2* Gene Structure and Mutations.

Supplemental Figure 8. *FLY1* and *FLY2* May Be Involved in Xylem Development.

Supplemental Figure 9. Alignment of the RING-H2 Domains of FLY1, FLY2, and TUL1.

Supplemental Figure 10. Analysis of *FLY1*$_{pro}$*:FLY1-YFP* Expression in Developing Seeds.

Supplemental Figure 11. Wortmannin Induces Fusions of FLY1-YFP Punctae.

Supplemental Table 1. Gene-Specific Primers Used for T-DNA Genotyping and RT-PCR Analysis.

ACKNOWLEDGMENTS

We thank the staff of the University of British Columbia BioImaging Facility for invaluable help with microscopy. We are grateful for the assistance of Shawn Mansfield University of British Columbia (UBC) with monosaccharide analysis. Gabriel Lévesque-Tremblay (UBC) provided cDNA samples. The pAD vector was a gift from Allan DeBono (UBC). The *35S:ST-RFP* construct was a gift from Chris Hawes (Oxford Brookes University), and *35S:VHAa1-RFP* transgenic seeds were provided by Miki Fujita (University of British Columbia). We thank Diana Starr Young (UBC), Andrew Karpov (UBC), Golya Mirderikvand (UBC), Kuljit Dhaliwal (UBC), and Tiffany Ngai (UBC) for technical assistance with mapping. This research was funded by a Natural Sciences and Engineering Research Council of Canada Discovery Grant to G.W.H. and by a grant from the National Science Foundation (MCB 0929100), the Howard Hughes Medical Institute, and the Gordon and Betty Moore Foundation to M.E.

AUTHOR CONTRIBUTIONS

C.V. designed and conducted research, analyzed data, and wrote the article. G.H.D., J.S.G., K.K., and T.L.W. designed and conducted research and analyzed data. A.G., G.D., and Y.T.H. conducted research. M.E. designed research and analyzed data. G.W.H. designed research, analyzed data, and wrote the article.

Received November 27, 2012; revised February 14, 2013; accepted February 18, 2013; published March 12, 2013.

REFERENCES

Abramoff, M.D., Magalhaes, P.J., and Ram, S.J. (2004). Image Processing with ImageJ. Biophotonics Int. **11:** 36–42.

Alonso, J.M., et al. (2003). Genome-wide insertional mutagenesis of *Arabidopsis thaliana*. Science **301:** 653–657.

Anderson, C.T., Carroll, A., Akhmetova, L., and Somerville, C. (2010). Real-time imaging of cellulose reorientation during cell wall expansion in *Arabidopsis* roots. Plant Physiol. **152:** 787–796.

Arsovski, A.A., Popma, T.M., Haughn, G.W., Carpita, N.C., McCann, M.C., and Western, T.L. (2009). *AtBXL1* encodes a bifunctional β-D-xylosidase/α-L-arabinofuranosidase required for pectic arabinan modification in *Arabidopsis* mucilage secretory cells. Plant Physiol. **150:** 1219–1234.

Atmodjo, M.A., Sakuragi, Y., Zhu, X., Burrell, A.J., Mohanty, S.S., Atwood, J.A., III., Orlando, R., Scheller, H.V., and Mohnen, D. (2011). Galacturonosyltransferase (GAUT)1 and GAUT7 are the core of a plant cell wall pectin biosynthetic homogalacturonan:galacturonosyltransferase complex. Proc. Natl. Acad. Sci. USA **108:** 20225–20230.

Barberon, M., Zelazny, E., Robert, S., Conéjéro, G., Curie, C., Friml, J., and Vert, G. (2011). Monoubiquitin-dependent endocytosis of the iron-regulated transporter 1 (IRT1) transporter controls iron uptake in plants. Proc. Natl. Acad. Sci. USA **108:** E450–E458.

Bhargava, A., Ahad, A., Wang, S., Mansfield, S.D., Haughn, G.W., Douglas, C.J., and Ellis, B.E. (January 18, 2013). The interacting MYB75 and KNAT7 transcription factors modulate secondary cell wall deposition both in stems and seed coat in *Arabidopsis*. Planta, in press.

Batoko, H., Zheng, H.Q., Hawes, C., and Moore, I. (2000). A rab1 GTPase is required for transport between the endoplasmic reticulum and Golgi apparatus and for normal Golgi movement in plants. Plant Cell **12:** 2201–2218.

Beeckman, T., De Rycke, R., Viane, R., and Inzé, D. (2000). Histological study of seed coat development in *Arabidopsis thaliana*. J. Plant Res. **V113:** 139–148.

Brady, S.M., Orlando, D.A., Lee, J.-Y., Wang, J.Y., Koch, J., Dinneny, J.R., Mace, D., Ohler, U., and Benfey, P.N. (2007). A high-resolution root spatiotemporal map reveals dominant expression patterns. Science **318:** 801–806.

Brandizzi, F., Fricker, M., and Hawes, C. (2002). A greener world: The revolution in plant bioimaging. Nat. Rev. Mol. Cell Biol. **3:** 520–530.

Caffall, K.H., Pattathil, S., Phillips, S.E., Hahn, M.G., and Mohnen, D. (2009). *Arabidopsis thaliana* T-DNA mutants implicate GAUT genes in the biosynthesis of pectin and xylan in cell walls and seed testa. Mol. Plant **2:** 1000–1014.

Clough, S.J., and Bent, A.F. (1998). Floral dip: A simplified method for Agrobacterium-mediated transformation of *Arabidopsis thaliana*. Plant J. **16:** 735–743.

Dean, G.H., Zheng, H., Tewari, J., Huang, J., Young, D.S., Hwang, Y.T., Western, T.L., Carpita, N.C., McCann, M.C., Mansfield, S.D., and Haughn, G.W. (2007). The *Arabidopsis MUM2* gene encodes a β-galactosidase required for the production of seed coat mucilage with correct hydration properties. Plant Cell **19:** 4007–4021.

DeBono, A.G. (2012). The Role and Behavior of *Arabidopsis thaliana* Lipid Transfer Proteins during Cuticular Wax Deposition. PhD dissertation (Vancouver, Canada: University of British Columbia).

Derbyshire, P., McCann, M.C., and Roberts, K. (2007). Restricted cell elongation in *Arabidopsis* hypocotyls is associated with a reduced average pectin esterification level. BMC Plant Biol. **7:** 31.

Dettmer, J., Hong-Hermesdorf, A., Stierhof, Y.D., and Schumacher, K. (2006). Vacuolar H+-ATPase activity is required for endocytic and secretory trafficking in *Arabidopsis*. Plant Cell **18:** 715–730.

Dowil, R.T., Lu, X., Saracco, S.A., Vierstra, R.D., and Downes, B.P. (2011). *Arabidopsis* membrane-anchored ubiquitin-fold (MUB) proteins localize a specific subset of ubiquitin-conjugating (E2) enzymes to the plasma membrane. J. Biol. Chem. **286:** 14913–14921.

Glickman, M.H., and Ciechanover, A. (2002). The ubiquitin-proteasome proteolytic pathway: destruction for the sake of construction. Physiol. Rev. **82:** 373–428.

Goldberg, R., Morvan, C., Jauneau, A., and Jarvis, M.C. (1996). Methyl-esterification, de-esterification and gelation of pectins in the primary cell wall. In Pectins and Pectinases, Visser J., Voragen A.G.J., eds (Amsterdam: Elsevier Science BV), pp. 151–172.

Goodstein, D.M., Shu, S., Howson, R., Neupane, R., Hayes, R.D., Fazo, J., Mitros, T., Dirks, W., Hellsten, U., Putnam, N., and Rokhsar, D.S. (2012). Phytozome: A comparative platform for green plant genomics. Nucleic Acids Res. **40** (Database issue)**:** D1178–D1186.

Hamilton, J.M.U., Simpson, D.J., Hyman, S.C., Ndimba, B.K., and Slabas, A.R. (2003). Ara12 subtilisin-like protease from *Arabidopsis thaliana*: Purification, substrate specificity and tissue localization. Biochem. J. **370:** 57–67.

Hardtke, C.S., Okamoto, H., Stoop-Myer, C., and Deng, X.W. (2002). Biochemical evidence for ubiquitin ligase activity of the *Arabidopsis* COP1 interacting protein 8 (CIP8). Plant J. **30:** 385–394.

Harholt, J., Suttangkakul, A., and Vibe Scheller, H. (2010). Biosynthesis of pectin. Plant Physiol. **153:** 384–395.

Harpaz-Saad, S., McFarlane, H.E., Xu, S., Divi, U.K., Forward, B., Western, T.L., and Kieber, J.J. (2011). Cellulose synthesis via the FEI2 RLK/SOS5 pathway and cellulose synthase 5 is required for the structure of seed coat mucilage in *Arabidopsis*. Plant J. **68:** 941–953.

Haughn, G.W., and Somerville, C. (1986). Sulfonylurea-resistant mutants of *Arabidopsis thaliana*. Mol. Gen. Genet. **204:** 430–434.

Haughn, G.W., and Western, T.L. (2012). *Arabidopsis* seed coat mucilage is a specialized cell wall that can be used as a model for genetic analysis of plant cell wall structure and function. Front. Plant Sci. **3:** 64.

Held, M.A., Be, E., Zemelis, S., Withers, S., Wilkerson, C., and Brandizzi, F. (2011). CGR3: A Golgi-localized protein influencing homogalacturonan methylesterification. Mol. Plant **4:** 832–844.

Hellens, R.P., Edwards, E.A., Leyland, N.R., Bean, S., and Mullineaux, P.M. (2000). pGreen: A versatile and flexible binary Ti vector for Agrobacterium-mediated plant transformation. Plant Mol. Biol. **42:** 819–832.

Hicke, L., and Dunn, R. (2003). Regulation of membrane protein transport by ubiquitin and ubiquitin-binding proteins. Annu. Rev. Cell Dev. Biol. **19:** 141–172.

Hruz, T., Laule, O., Szabo, G., Wessendorp, F., Bleuler, S., Oertle, L., Widmayer, P., Gruissem, W., and Zimmermann, P. (2008). Genevestigator v3: A reference expression database for the meta-analysis of transcriptomes. Adv. Bioinforma. **2008:** 420747.

Huang, X., and Miller, W. (1991). A time-efficient linear-space local similarity algorithm. Adv. Appl. Math. **12:** 337–357.

Jander, G., Norris, S.R., Rounsley, S.D., Bush, D.F., Levin, I.M., and Last, R.L. (2002). *Arabidopsis* map-based cloning in the post-genome era. Plant Physiol. **129:** 440–450.

Jarvis, M.C. (1984). Structure and properties of pectin gels in plant cell walls. Plant Cell Environ. **7:** 153–164.

Jolie, R.P., Duvetter, T., Van Loey, A.M., and Hendrickx, M.E. (2010). Pectin methylesterase and its proteinaceous inhibitor: A review. Carbohydr. Res. **345:** 2583–2595.

Kasajima, I., Ide, Y., Ohkama-Ohtsu, N., Hayashi, H., Yoneyama, T., and Fujiwara, T. (2004). A protocol for rapid DNA extraction from *Arabidopsis thaliana* for PCR analysis. Plant Mol. Biol. Rep. **22:** 49–52.

Klavons, J.A., and Bennett, R.D. (1986). Determination of methanol using alcohol oxidase and its application to methyl ester content of pectins. J. Agric. Food Chem. **34:** 597–599.

Knox, J.P. (1997). The use of antibodies to study the architecture and developmental regulation of plant cell walls. Int. Rev. Cytol. **171:** 79–120.

Knox, J.P., Linstead, P.J., King, J., Cooper, C., and Roberts, K. (1990). Pectin esterification is spatially regulated both within cell walls and between developing tissues of root apices. Planta **181:** 512–521.

Krupková, E., Immerzeel, P., Pauly, M., and Schmülling, T. (2007). The *TUMOROUS SHOOT DEVELOPMENT2* gene of *Arabidopsis* encoding a putative methyltransferase is required for cell adhesion and co-ordinated plant development. Plant J. **50:** 735–750.

Lamesch, P., et al. (2012). The Arabidopsis Information Resource (TAIR): Improved gene annotation and new tools. Nucleic Acids Res. **40** (Database issue)**:** D1202–D1210.

Larkin, M.A., et al. (2007). Clustal W and Clustal X version 2.0. Bioinformatics **23:** 2947–2948.

Le, B.H., et al. (2010). Global analysis of gene activity during *Arabidopsis* seed development and identification of seed-specific transcription factors. Proc. Natl. Acad. Sci. USA **107:** 8063–8070.

Lee, M.H., Min, M.K., Lee, Y.J., Jin, J.B., Shin, D.H., Kim, D.H., Lee, K.-H., and Hwang, I. (2002). ADP-ribosylation factor 1 of *Arabidopsis* plays a critical role in intracellular trafficking and maintenance of endoplasmic reticulum morphology in *Arabidopsis*. Plant Physiol. **129:** 1507–1520.

Liners, F., Letesson, J.J., Didembourg, C., and Van Cutsem, P. (1989). Monoclonal antibodies against pectin: Recognition of a conformation induced by calcium. Plant Physiol. **91:** 1419–1424.

Lionetti, V., Raiola, A., Camardella, L., Giovane, A., Obel, N., Pauly, M., Favaron, F., Cervone, F., and Bellincampi, D. (2007). Overexpression of pectin methylesterase inhibitors in *Arabidopsis* restricts fungal infection by *Botrytis cinerea*. Plant Physiol. **143:** 1871–1880.

Lord, E.M., and Mollet, J.-C. (2002). Plant cell adhesion: A bioassay facilitates discovery of the first pectin biosynthetic gene. Proc. Natl. Acad. Sci. USA **99:** 15843–15845.

Macquet, A., Ralet, M.-C., Kronenberger, J., Marion-Poll, A., and North, H.M. (2007a). In situ, chemical and macromolecular study of the composition of *Arabidopsis thaliana* seed coat mucilage. Plant Cell Physiol. **48:** 984–999.

MacGurn, J.A., Hsu, P.C., and Emr, S.D. (2012). Ubiquitin and membrane protein turnover: From cradle to grave. Annu. Rev. Biochem. **81:** 231–259.

Macquet, A., Ralet, M.-C., Loudet, O., Kronenberger, J., Mouille, G., Marion-Poll, A., and North, H.M. (2007b). A naturally occurring

mutation in an *Arabidopsis* accession affects a beta-D-galactosidase that increases the hydrophilic potential of rhamnogalacturonan I in seed mucilage. Plant Cell **19:** 3990–4006.

Mareck, A., Lamour, R., Schaumann, A., Chan, P., Driouich, A., Pelloux, J., and Lerouge, P. (2012). Analysis of LuPME3, a pectin methylesterase from *Linum usitatissimum*, revealed a variability in PME proteolytic maturation. Plant Signal. Behav. **7:** 59–61.

Mendu, V., Griffiths, J.S., Persson, S., Stork, J., Downie, A.B., Voiniciuc, C., Haughn, G.W., and DeBolt, S. (2011). Subfunctionalization of cellulose synthases in seed coat epidermal cells mediates secondary radial wall synthesis and mucilage attachment. Plant Physiol. **157:** 441–453.

Miao, Y., Li, H.-Y., Shen, J., Wang, J., and Jiang, L. (2011). QUASIMODO 3 (QUA3) is a putative homogalacturonan methyltransferase regulating cell wall biosynthesis in *Arabidopsis* suspension-cultured cells. J. Exp. Bot. **62:** 5063–5078.

Micheli, F. (2001). Pectin methylesterases: Cell wall enzymes with important roles in plant physiology. Trends Plant Sci. **6:** 414–419.

Mohnen, D. (2008). Pectin structure and biosynthesis. Curr. Opin. Plant Biol. **11:** 266–277.

Mouille, G., Ralet, M.-C., Cavelier, C., Eland, C., Effroy, D., Hématy, K., McCartney, L., Truong, H.N., Gaudon, V., Thibault, J.-F., Marchant, A., and Höfte, H. (2007). Homogalacturonan synthesis in *Arabidopsis thaliana* requires a Golgi-localized protein with a putative methyltransferase domain. Plant J. **50:** 605–614.

Moustacas, A.M., Nari, J., Borel, M., Noat, G., and Ricard, J. (1991). Pectin methylesterase, metal ions and plant cell-wall extension. The role of metal ions in plant cell-wall extension. Biochem. J. **279:** 351–354.

Müller, J., Mettbach, U., Menzel, D., and Samaj, J. (2007). Molecular dissection of endosomal compartments in plants. Plant Physiol. **145:** 293–304.

Mutwil, M., Debolt, S., and Persson, S. (2008). Cellulose synthesis: A complex complex. Curr. Opin. Plant Biol. **11:** 252–257.

Obayashi, T., Nishida, K., Kasahara, K., and Kinoshita, K. (2011). ATTED-II updates: Condition-specific gene coexpression to extend coexpression analyses and applications to a broad range of flowering plants. Plant Cell Physiol. **52:** 213–219.

Oka, T., Nemoto, T., and Jigami, Y. (2007). Functional analysis of *Arabidopsis thaliana* RHM2/MUM4, a multidomain protein involved in UDP-D-glucose to UDP-L-rhamnose conversion. J. Biol. Chem. **282:** 5389–5403.

Ostlund, G., Schmitt, T., Forslund, K., Köstler, T., Messina, D.N., Roopra, S., Frings, O., and Sonnhammer, E.L.L. (2010). InParanoid 7: New algorithms and tools for eukaryotic orthology analysis. Nucleic Acids Res. **38** (Database issue)**:** D196–D203.

Pattathil, S., et al. (2010). A comprehensive toolkit of plant cell wall glycan-directed monoclonal antibodies. Plant Physiol. **153:** 514–525.

Pelloux, J., Rustérucci, C., and Mellerowicz, E.J. (2007). New insights into pectin methylesterase structure and function. Trends Plant Sci. **12:** 267–277.

Penfield, S., Meissner, R.C., Shoue, D.A., Carpita, N.C., and Bevan, M.W. (2001). MYB61 is required for mucilage deposition and extrusion in the *Arabidopsis* seed coat. Plant Cell **13:** 2777–2791.

Petersen, T.N., Brunak, S., von Heijne, G., and Nielsen, H. (2011). SignalP 4.0: Discriminating signal peptides from transmembrane regions. Nat. Methods **8:** 785–786.

Quevillon, E., Silventoinen, V., Pillai, S., Harte, N., Mulder, N., Apweiler, R., and Lopez, R. (2005). InterProScan: protein domains identifier. Nucleic Acids Res. **33** (Web Server issue)**:** W116–W120.

Rautengarten, C., Usadel, B., Neumetzler, L., Hartmann, J., Büssis, D., and Altmann, T. (2008). A subtilisin-like serine protease essential for mucilage release from *Arabidopsis* seed coats. Plant J. **54:** 466–480.

Reggiori, F., and Pelham, H.R.B. (2002). A transmembrane ubiquitin ligase required to sort membrane proteins into multivesicular bodies. Nat. Cell Biol. **4:** 117–123.

Rensing, K.H., Samuels, A.L., and Savidge, R.A. (2002). Ultrastructure of vascular cambial cell cytokinesis in pine seedlings preserved by cryofixation and substitution. Protoplasma **220:** 39–49.

Robinson, D.G., Langhans, M., Saint-Jore-Dupas, C., and Hawes, C. (2008). BFA effects are tissue and not just plant specific. Trends Plant Sci. **13:** 405–408.

Romano, J.M., et al. (2012). AtMYB61, an R2R3-MYB transcription factor, functions as a pleiotropic regulator via a small gene network. New Phytol. **195:** 774–786.

Saint-Jore-Dupas, C., Gomord, V., and Paris, N. (2004). Protein localization in the plant Golgi apparatus and the trans-Golgi network. Cell. Mol. Life Sci. **61:** 159–171.

Schmid, M., Davison, T.S., Henz, S.R., Pape, U.J., Demar, M., Vingron, M., Schölkopf, B., Weigel, D., and Lohmann, J.U. (2005). A gene expression map of *Arabidopsis thaliana* development. Nat. Genet. **37:** 501–506.

Schnell, J.D., and Hicke, L. (2003). Non-traditional functions of ubiquitin and ubiquitin-binding proteins. J. Biol. Chem. **278:** 35857–35860.

Schwacke, R., Schneider, A., van der Graaff, E., Fischer, K., Catoni, E., Desimone, M., Frommer, W.B., Flügge, U.-I., and Kunze, R. (2003). ARAMEMNON, a novel database for *Arabidopsis* integral membrane proteins. Plant Physiol. **131:** 16–26.

Sigrist, C.J.A., Cerutti, L., de Castro, E., Langendijk-Genevaux, P.S., Bulliard, V., Bairoch, A., and Hulo, N. (2010). PROSITE, a protein domain database for functional characterization and annotation. Nucleic Acids Res. **38** (Database issue)**:** D161–D166.

Sriamornsak, S. (2003). Chemistry of pectin and its pharmaceutical uses: A review. Silpakorn University International Journal. **3:** 206–228.

Sterling, C. (1970). Crystal-structure of ruthenium red and stereochemistry of its pectic stain. Am. J. Bot. **57:** 172–175.

Sterling, J.D., Atmodjo, M.A., Inwood, S.E., Kumar Kolli, V.S., Quigley, H.F., Hahn, M.G., and Mohnen, D. (2006). Functional identification of an *Arabidopsis* pectin biosynthetic homogalacturonan galacturonosyltransferase. Proc. Natl. Acad. Sci. USA **103:** 5236–5241.

Saez-Aguayo, S., Ralet, M.C., Berger, A., Botran, L., Ropartz, D., Marion-Poll, A., and North, H.M. (2013). PECTIN METHYLESTERASE INHIBITOR6 promotes *Arabidopsis* mucilage release by limiting methylesterification of homogalacturonan in seed coat epidermal cells. Plant Cell **25:** 308–323.

Stone, S.L., Hauksdóttir, H., Troy, A., Herschleb, J., Kraft, E., and Callis, J. (2005). Functional analysis of the RING-type ubiquitin ligase family of *Arabidopsis*. Plant Physiol. **137:** 13–30.

Stork, J., Harris, D., Griffiths, J., Williams, B., Beisson, F., Li-Beisson, Y., Mendu, V., Haughn, G., and Debolt, S. (2010). CELLULOSE SYNTHASE9 serves a nonredundant role in secondary cell wall synthesis in *Arabidopsis* epidermal testa cells. Plant Physiol. **153:** 580–589.

Sullivan, S., Ralet, M.-C., Berger, A., Diatloff, E., Bischoff, V., Gonneau, M., Marion-Poll, A., and North, H.M. (2011). CESA5 is required for the synthesis of cellulose with a role in structuring the adherent mucilage of *Arabidopsis* seeds. Plant Physiol. **156:** 1725–1739.

Usadel, B., Kuschinsky, A.M., Rosso, M.G., Eckermann, N., and Pauly, M. (2004). RHM2 is involved in mucilage pectin synthesis

and is required for the development of the seed coat in *Arabidopsis*. Plant Physiol. **134:** 286–295.

Van Bel, M., Proost, S., Wischnitzki, E., Movahedi, S., Scheerlinck, C., Van de Peer, Y., and Vandepoele, K. (2012). Dissecting plant genomes with the PLAZA comparative genomics platform. Plant Physiol. **158:** 590–600.

Vandenbosch, K.A., Bradley, D.J., Knox, J.P., Perotto, S., Butcher, G.W., and Brewin, N.J. (1989). Common components of the infection thread matrix and the intercellular space identified by immunocytochemical analysis of pea nodules and uninfected roots. EMBO J. **8:** 335–341.

van den Hoogen, B.M., van Weeren, P.R., Lopes-Cardozo, M., van Golde, L.M.G., Barneveld, A., and van de Lest, C.H.A. (1998). A microtiter plate assay for the determination of uronic acids. Anal. Biochem. **257:** 107–111.

Verollet, R. (2008). A major step towards efficient sample preparation with bead-beating. Biotechniques **44:** 832–833.

Viotti, C., et al. (2010). Endocytic and secretory traffic in *Arabidopsis* merge in the trans-Golgi network/early endosome, an independent and highly dynamic organelle. Plant Cell **22:** 1344–1357.

Wang, J., Cai, Y., Miao, Y., Lam, S.K., and Jiang, L. (2009). Wortmannin induces homotypic fusion of plant prevacuolar compartments. J. Exp. Bot. **60:** 3075–3083.

Western, T.L., Burn, J., Tan, W.L., Skinner, D.J., Martin-McCaffrey, L., Moffatt, B.A., and Haughn, G.W. (2001). Isolation and characterization of mutants defective in seed coat mucilage secretory cell development in *Arabidopsis*. Plant Physiol. **127:** 998–1011.

Western, T.L., Skinner, D.J., and Haughn, G.W. (2000). Differentiation of mucilage secretory cells of the *Arabidopsis* seed coat. Plant Physiol. **122:** 345–356.

Western, T.L., Young, D.S., Dean, G.H., Tan, W.L., Samuels, A.L., and Haughn, G.W. (2004). *MUCILAGE-MODIFIED4* encodes a putative pectin biosynthetic enzyme developmentally regulated by *APETALA2*, *TRANSPARENT TESTA GLABRA1*, and *GLABRA2* in the *Arabidopsis* seed coat. Plant Physiol. **134:** 296–306.

Windsor, J.B., Symonds, V.V., Mendenhall, J., and Lloyd, A.M. (2000). *Arabidopsis* seed coat development: Morphological differentiation of the outer integument. Plant J. **22:** 483–493.

Willats, W.G., McCartney, L., Mackie, W., and Knox, J.P. (2001a). Pectin: Cell biology and prospects for functional analysis. Plant Mol. Biol. **47:** 9–27.

Willats, W.G.T., McCartney, L., and Knox, J.P. (2001b). In-situ analysis of pectic polysaccharides in seed mucilage and at the root surface of *Arabidopsis thaliana*. Planta **213:** 37–44.

Willats, W.G.T., Orfila, C., Limberg, G., Buchholt, H.C., van Alebeek, G.-J.W.M., Voragen, A.G.J., Marcus, S.E., Christensen, T.M.I.E., Mikkelsen, J.D., Murray, B.S., and Knox, J.P. (2001c). Modulation of the degree and pattern of methyl-esterification of pectic homogalacturonan in plant cell walls. Implications for pectin methyl esterase action, matrix properties, and cell adhesion. J. Biol. Chem. **276:** 19404–19413.

Winter, D., Vinegar, B., Nahal, H., Ammar, R., Wilson, G.V., and Provart, N.J. (2007). An "Electronic Fluorescent Pictograph" browser for exploring and analyzing large-scale biological data sets. PLoS ONE **2:** e718.

Wolf, S., Mouille, G., and Pelloux, J. (2009a). Homogalacturonan methyl-esterification and plant development. Mol. Plant **2:** 851–860.

Wolf, S., Rausch, T., and Greiner, S. (2009b). The N-terminal pro region mediates retention of unprocessed type-I PME in the Golgi apparatus. Plant J. **58:** 361–375.

Xu, C., Zhao, L., Pan, X., and Šamaj, J. (2011). Developmental localization and methylesterification of pectin epitopes during somatic embryogenesis of banana (*Musa* spp. AAA). PLoS ONE **6:** e22992.

Young, R.E., McFarlane, H.E., Hahn, M.G., Western, T.L., Haughn, G.W., and Samuels, A.L. (2008). Analysis of the Golgi apparatus in *Arabidopsis* seed coat cells during polarized secretion of pectin-rich mucilage. Plant Cell **20:** 1623–1638.

Zhang, G.F., and Staehelin, L.A. (1992). Functional compartmentation of the Golgi apparatus of plant cells: Immunocytochemical analysis of high-pressure frozen- and freeze-substituted sycamore maple suspension culture cells. Plant Physiol. **99:** 1070–1083.

Zimmermann, P., Hirsch-Hoffmann, M., Hennig, L., and Gruissem, W. (2004). GENEVESTIGATOR. *Arabidopsis* microarray database and analysis toolbox. Plant Physiol. **136:** 2621–2632.

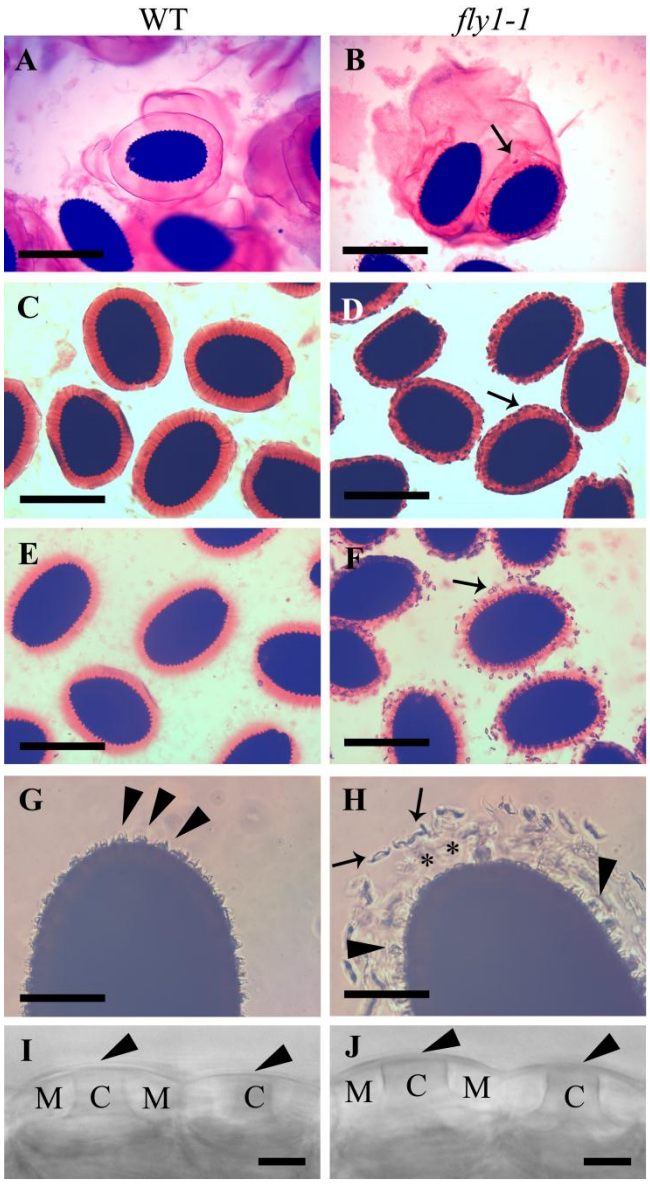

Supplemental Figure 1. Analysis of *fly1-1* Mucilage Extrusion and Primary Wall Attachment.

(A) and **(B)** Mature seeds hydrated in RR, without mechanical agitation. Both wild type (WT) and *fly1-1* release large amounts of non-adherent mucilage.
(C) and **(D)** Mature seeds shaken directly in RR. The *fly1-1* seeds display discs and a smaller mucilage capsule than WT.
(E) and **(F)** Mature seeds shaken in water for 24 h and then stained with RR. The inner, adherent mucilage layer and the *fly1-1* discs remain attached to seeds.
(G) and **(H)** Phase contrast micrographs of seeds shaken in water. Unlike *fly1-1*, all WT seed coat epidermal cells have primary cell walls attached to their columellae (arrowheads). The *fly1-1* seeds display discs (arrows) and loss of primary wall attachment (asterisks).
(I) and **(J)** Transmitted light images of live seed coat epidermal cells at 12 DPA. Both WT and *fly1-1* display primary cell walls (arrowheads) in close association with the columellae (C) during development. M, mucilage pockets.

Bars = 500 µm in **(A)** to **(F)**, 150 µm in **(G)** and **(H)**, and 10 µm in **(I)** and **(J)**.

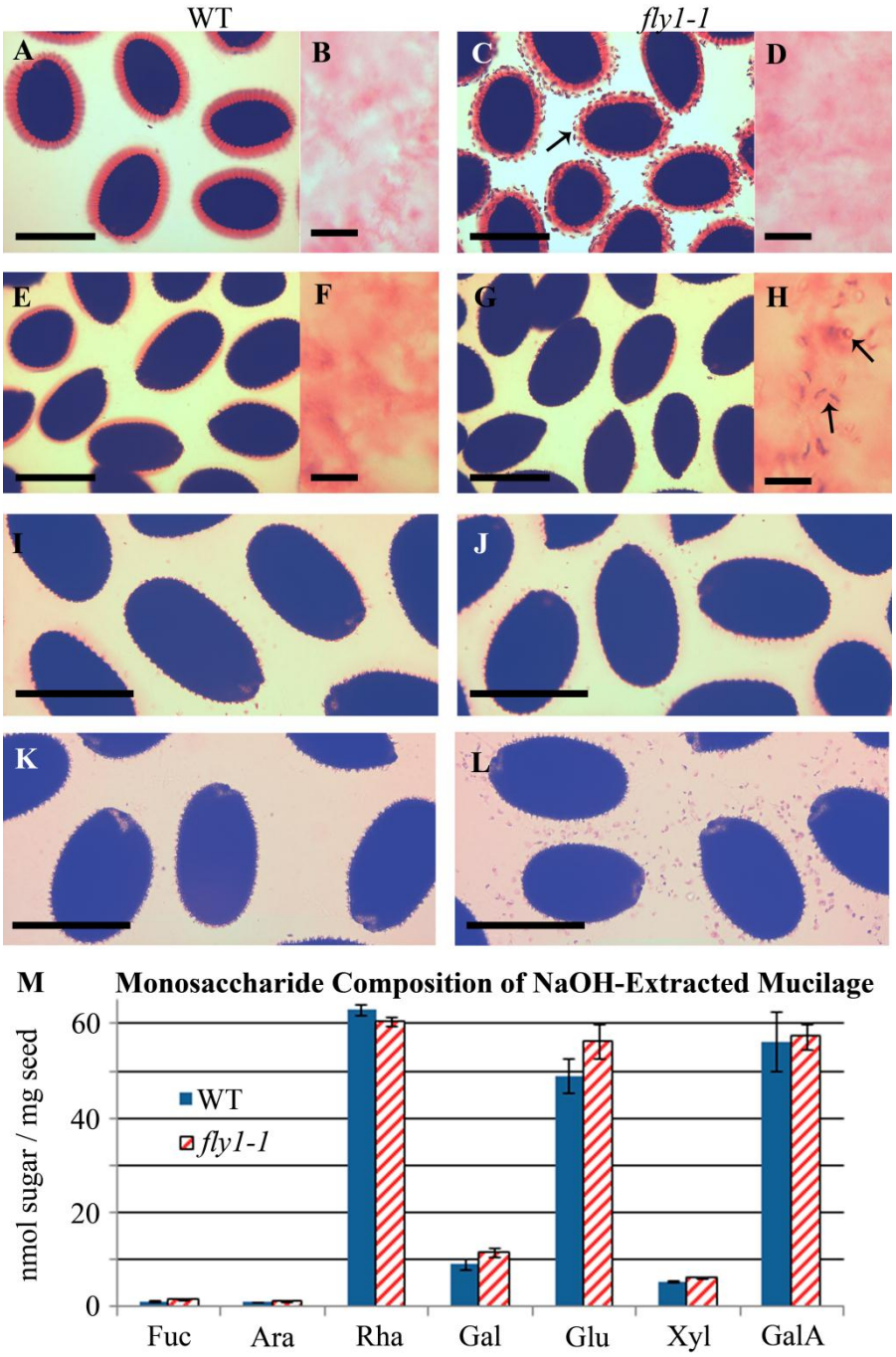

Supplemental Figure 2. Mucilage Extractions and Total Monosaccharide Composition.

(A) to **(L)** RR-staining of mucilage extractions for biochemical analysis. For sequential water extractions, seeds were gently shaken for 1 h **(A)** and **(C)**, or vortexed for an additional 2 h **(E)** and **(G)**. RR-stained extracted mucilage is shown in **(B)**, **(D)**, **(F)** and **(H)**. Discs (arrows) are removed from *fly1-1* seeds only after vigorous shaking.
(I) and **(J)** For DM analysis, seeds vortexed in 50 mM EDTA pH 8 for 1 h.
(K) and **(L)** Seeds vortexed in 0.2 NaOH for 1 h to remove all mucilage.
(M) Monosaccharide levels in wild type (WT) and *fly1-1* mucilage extracted from **(K)** and **(L)** respectively.. Values are the mean ± SE of four samples.Results were verified using two additional biological replicates.
Bars = 100 µm in **(B)**, **(D)**, **(F)** and **(H)**, and 500 µm in the other panels.

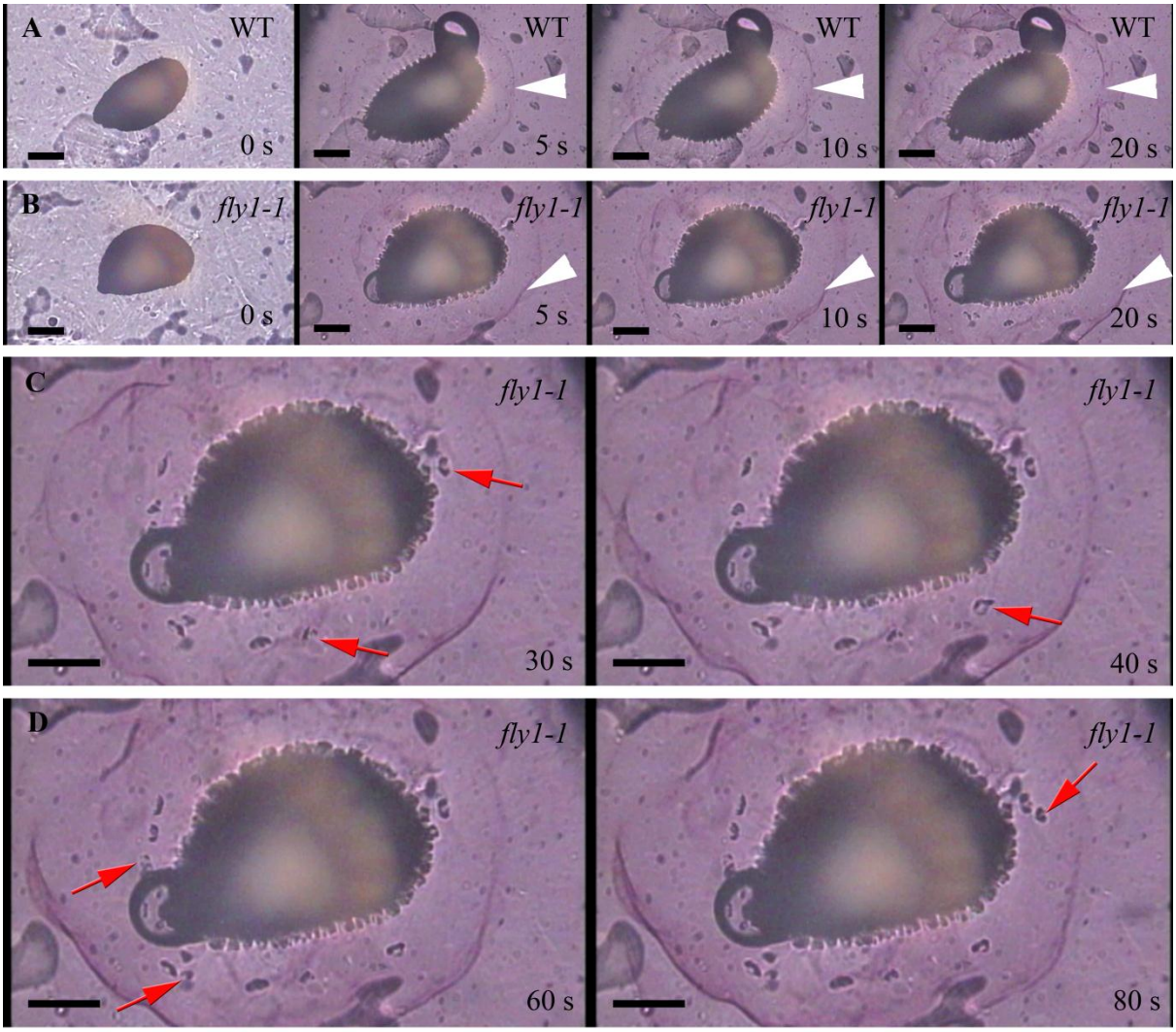

Supplemental Figure 3. Time Course Analysis of Mucilage Release From Seeds Upon Hydration.

(A) Wild type (WT) seed releases a large mucilage halo (arrowheads) within 10 s of hydration in RR. **(B)** to **(D)** *fly1-1* seed releases an equally large mucilage halo (arrowheads) within 10 s, but discs continue to be released after more than 60 s (arrows). Bars = 150 µm.

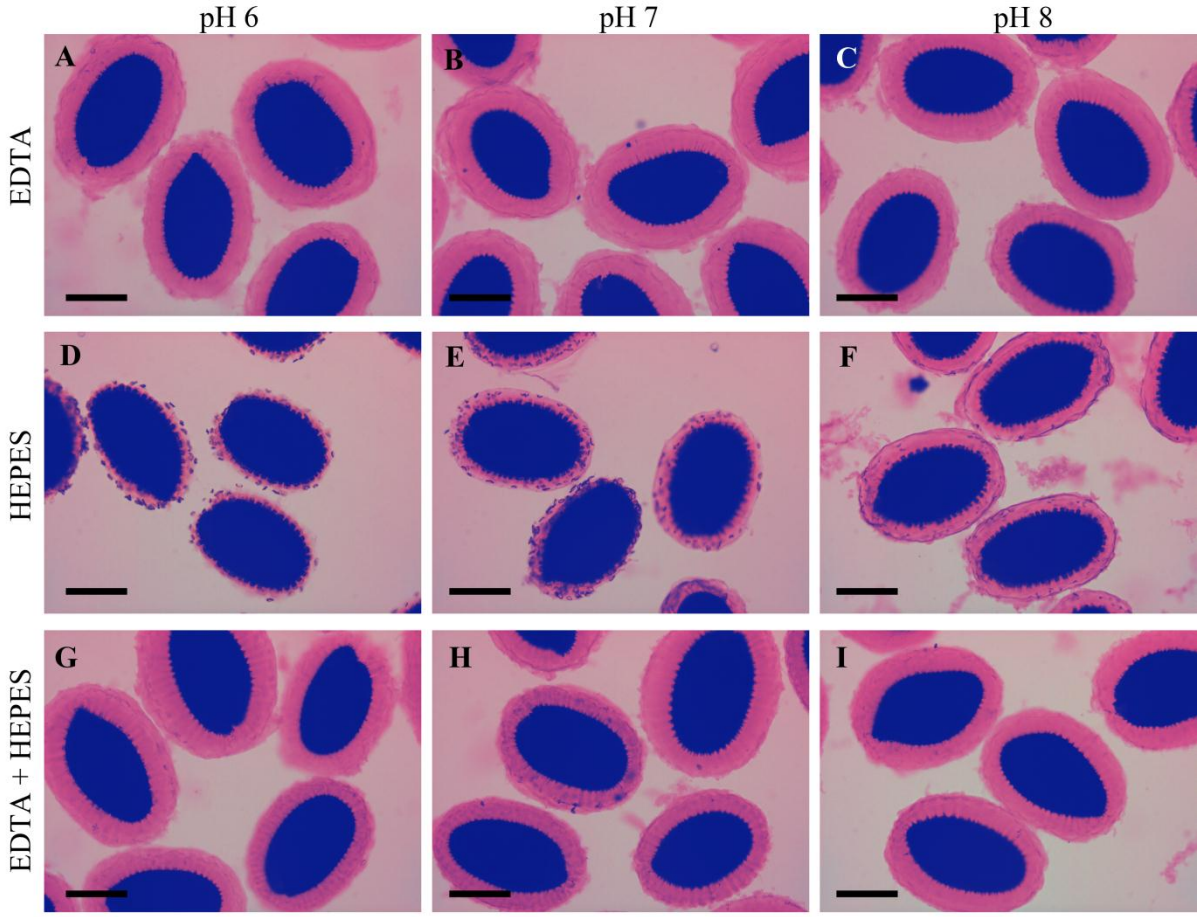

Supplemental Figure 4. Analysis of the Effect of Buffer pH on *fly1-1* Mucilage Defects.

(A) to **(I)** *fly1-1* seeds were shaken in 50 mM EDTA, 50 mM HEPES or both for 1 h before being rinsed and stained with RR.Unlike EDTA, HEPES does not chelate Ca^{2+} ions. EDTA pH 6 and 7 treatments **(A)** and **(B)** resemble the EDTA pH 8 treatment, which fully rescues the *fly1-1* mucilage defects **(C)**. HEPES partially rescues the defects at pH 8 **(F)** but not at pH 6 **(D)**. HEPES pH 7 shows an intermediate phenotype **(E)**. The EDTA + HEPES treatments **(G)** to **(I)** phenocopy the EDTA treatments **(A)** to **(C)**. Bars = 150 µm.

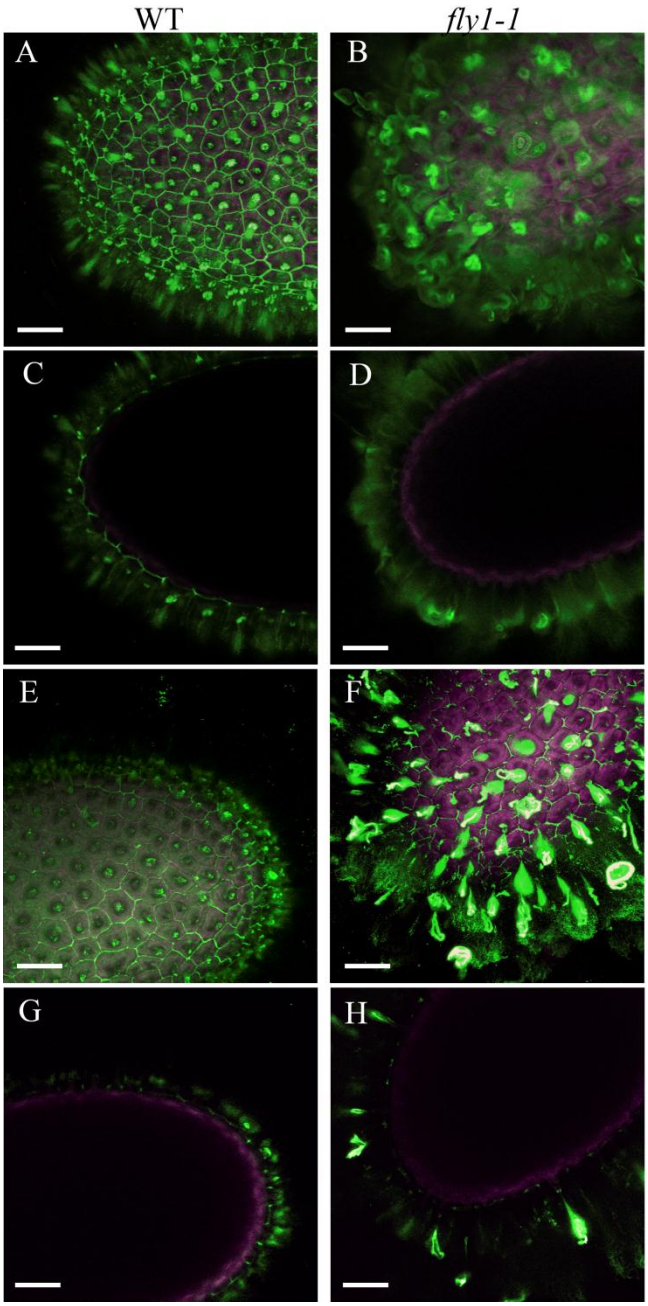

Supplemental Figure 5. Immunolabeling of Partially Methylesterified HG in Seeds.

(A) to **(D)** JIM5 and **(E)** to **(H)** JIM7 antibody signals are shown in green, and intrinsic seed fluorescence in magenta. **(A)**, **(B)**, **(E)** and **(F)** Maximum intensity signals from multiple optical slices. **(C)**, **(D)**, **(G)** and **(H)** represent single optical sections through the middle of seeds. JIM5 binds to low DM (up to 40%) HG (VandenBosch et al., 1989), and JIM7 labels high DM (35 to 81%) HG (Knox et al., 1990). The mucilage of *fly1-1* displays increased JIM5 and JIM7 immunofluorescence compared to wild type (WT). Bars = 50 µm.

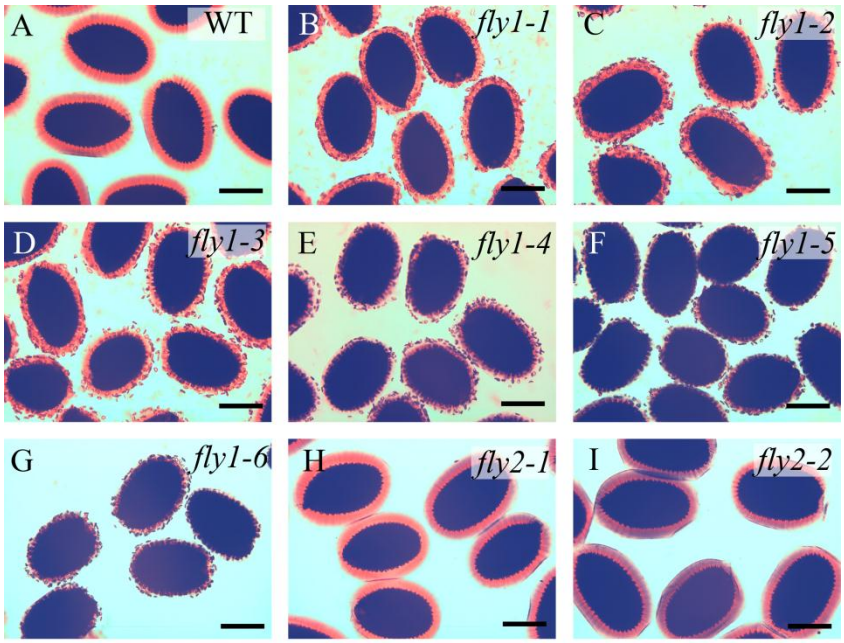

Supplemental Figure 6. Analysis of *fly1* and *fly2* Mucilage Extrusion.

(A) to **(I)** Seeds were shaken in water for 2 h and stained with RR. All *fly1* mutants have discs at the edge of the extruded mucilage. Wild type (WT) and *fly2* are indistinguishable. Bars = 300 µm.

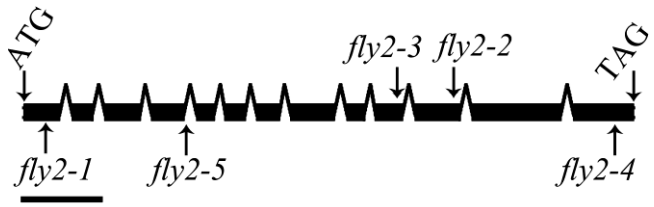

Supplemental Figure 7. *FLY2* Gene Structure and Mutations.

T-DNA insertions (*fly2-1* to *fly2-5*) are indicated with arrows. Boxes and connecting lines represent exons and introns. Bar = 300 amino acids.

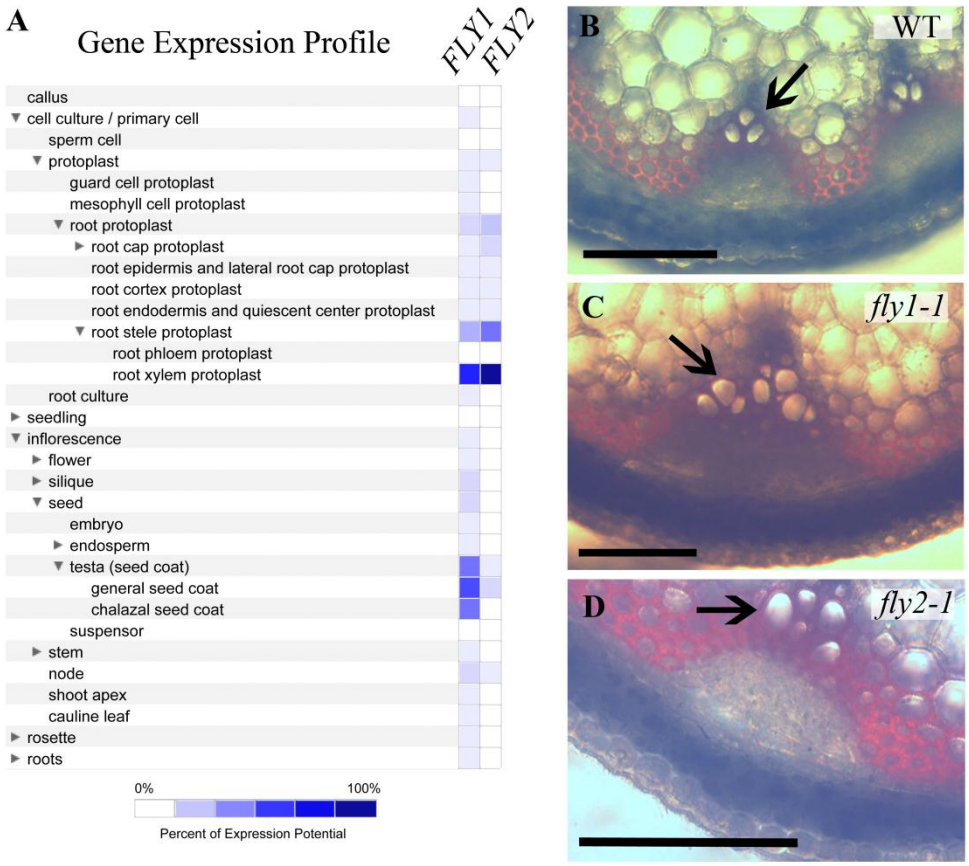

Supplemental Figure 8. *FLY1* and *FLY2* May Be Involved in Xylem Development.

(A) *FLY1* and *FLY2* are expressed highest in xylem cells. Relative transcript levels across Arabidopsis tissues and cell types are shown using a GENEVESTIGATOR heat map (Hruz et al., 2008). Values are normalized to the maximum expression level (darkest blue color) recorded for each gene. *FLY1*, unlike *FLY2*, also shows strong expression in the seed coat.
(B) to **(D)** Wild type (WT), *fly1-1*, and *fly2-1* display similar xylem cell morphology. Hand sections from the base of stems were stained with phloroglucinol-HCl. Arrows indicate xylem cells. Bars = 100 µm.

```
FLY1  504 CVICMTAIDL-------RQHTS--DCMVTPCEHFFHSGCLQRWMDIKMECPTCRRSLPP 561
FLY2  501 CVICMTTIDL-------RHRIN--DCMVTPCEHIFHSGCLQRWMDIKMECPTCRRPLPP 558
TUL1  698 CAICMSDVPIYIEEIPETHKVDQHSYMVTPCNHVFHTSCLENWMNYKLQCPVCRSPLPP 757
          *.***: : :         :: .   . *****:*.**:.**:.**: *::**.** .***
```

Supplemental Figure 9. Alignment of the RING-H2 domains of FLY1, FLY2 and TUL1.

Shading indicates the eight conserved Cys (C) and His (H) amino acids that define the RING-H2 domain (Stone et al., 2005). Fully conserved residues are indicated by an asterisk. A colon denotes conservation between groups with strongly similar properties, while a period indicates groups with weakly similar properties.

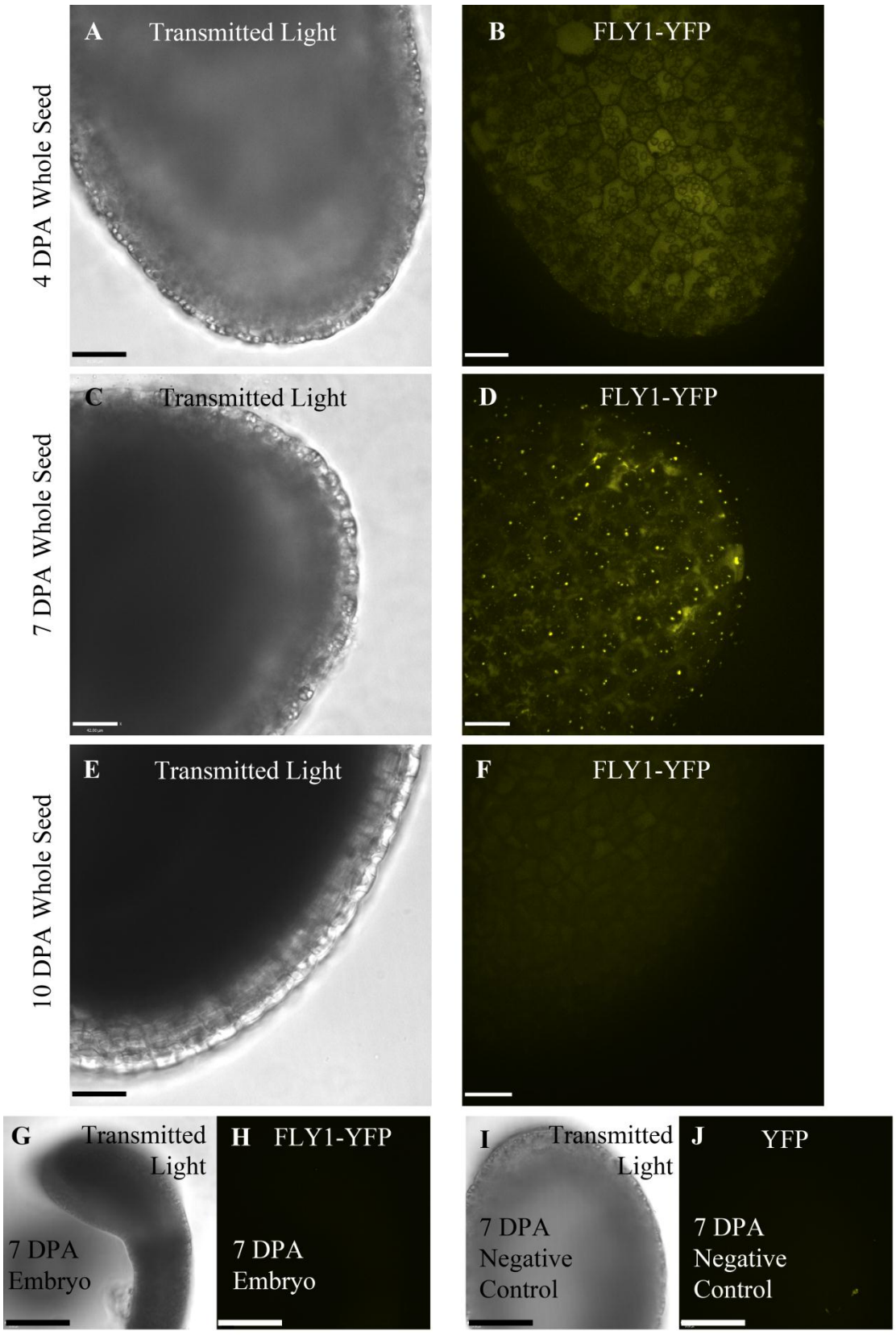

Supplemental Figure 10. Analysis of *FLY1*$_{pro}$:*FLY1-YFP* expression in developing seeds.

(A) to **(J)** Light micrographs of developing seed tissues, left of the corresponding YFP signals (maximum intensity signals from multiple stacks).
(A) to **(H)** *fly1-1* seeds rescued with the *FLY1*$_{pro}$:*FLY1-YFP* transgene show the highest FLY1-YFP expression in the seed coat epidermis at 7 DPA **(D)**, but not in the embryo **(H)**.
(J) 7 DPA *fly1-1* seeds without the *FLY1*$_{pro}$:*FLY1-YFP* transgene show no YFP signal. Bars = 50 µm in **(A)** to **(F)**, 25 µm in **(G)** to **(J)**.

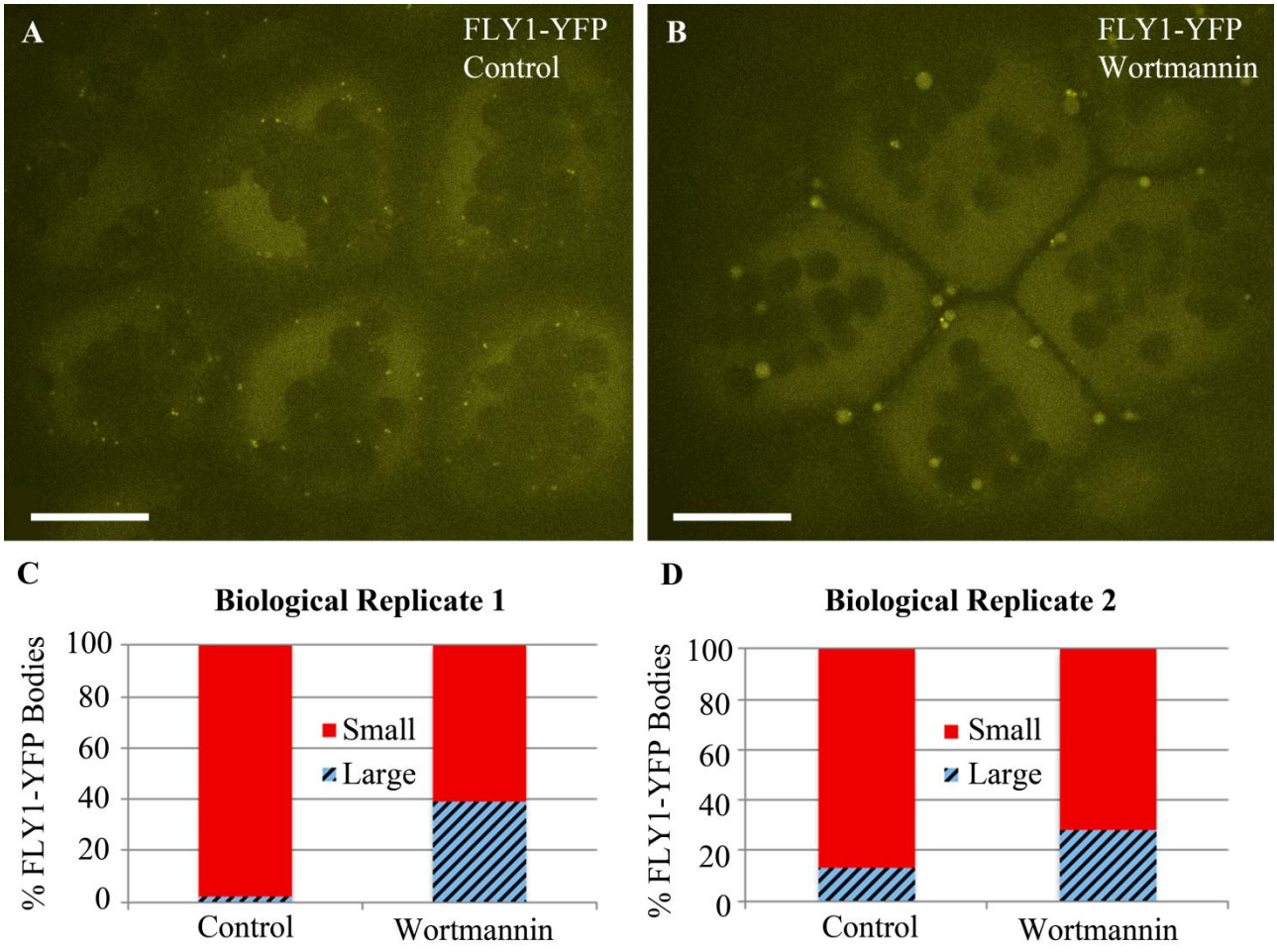

Supplemental Figure 11. Wortmannin Induces Fusions of FLY1-YFP punctae.

(A) and **(B)** *FLY1*$_{pro}$*:FLY1-YFP* seeds excised from the same 7 DPA silique. **(A)** Control seed displays many small punctae. **(B)** Seed treated with 20 µM wortmannin for 2 h displays many large bodies. Bars = 20 µm.
(C) and **(D)** Wortmannin induced the fusion of small FLY1-YFP punctae (0.1 µm^2 to 1.5 µm^2), thereby increasing the ratio of large bodies (2.5 µm^2 to 8 µm^2) to punctae. Approximately 200 punctae/bodies were counted in each of the two biological replicates.

Supplemental Table 1. Gene-Specific Primers Used for T-DNA Genotyping and RT-PCR Analysis.

Locus	**Left Primer (5' to 3')**	**Right Primer (5' to 3')**
fly1-2	CGCAAGTTCAGATGCTAATGC	AAAAAGGAACCGACAAACCTG
fly1-3	AGGCACAAATAAGCATCCATG	ATGAACAAAATGTGGGTGGTG
fly1-4	TCTGCTAATGGCTTGTTTGATG	ACGGGTTGCTTTCCATATAGC
fly1-5	TTTTCACTAGAAGCCACACGG	CTTGCAGTGGCTCTTTGGTAG
fly1-6	GCACTCAAGATTCAGTGCAGG	ATGACGGAGATTGTTTTTCCC
fly2-1	AACTGCACCCTGTTCACATTC	ACTCCGACATTCCAAGTTTCC
fly2-2	CGATTCCTAAGGAACCAAAGG	TTCTTGTATACAAGGGTGCCG
FLY1	TGTAGAGCCCAACAAGGTTTG	GATCAATAGCGGTCATGCAG
FLY2	CAAAAAAGAAAAAGGTGGAGCAG	AATTTTTGTTGGACTTGTCAC
GAPC	GATTCGGAAGAATTGGTCGTTT	CTTCAAGTGAGCTGCAGCCTT